CHAPTER 9

Phase Diagrams—Equilibrium Microstructural Development

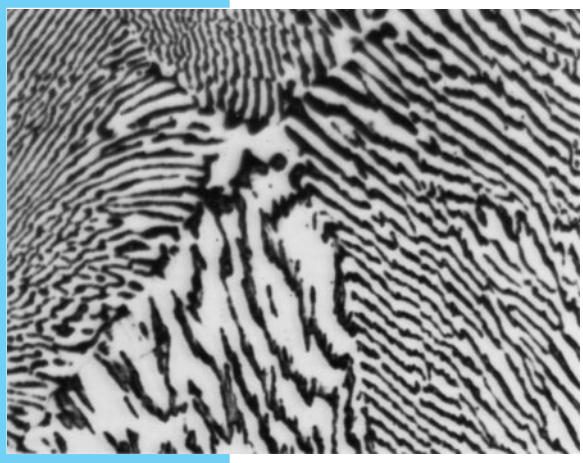

The microstructure of a slowly cooled "eutectic" soft solder (≈ 38 wt % Pb – wt % Sn) consists of a lamellar structure of tin-rich solid solution (white) and lead-rich solid solution (dark), 375X. (From ASM Handbook, Vol. 3: Alloy Phase Diagrams, ASM International, Materials Park, Ohio, 1992.)

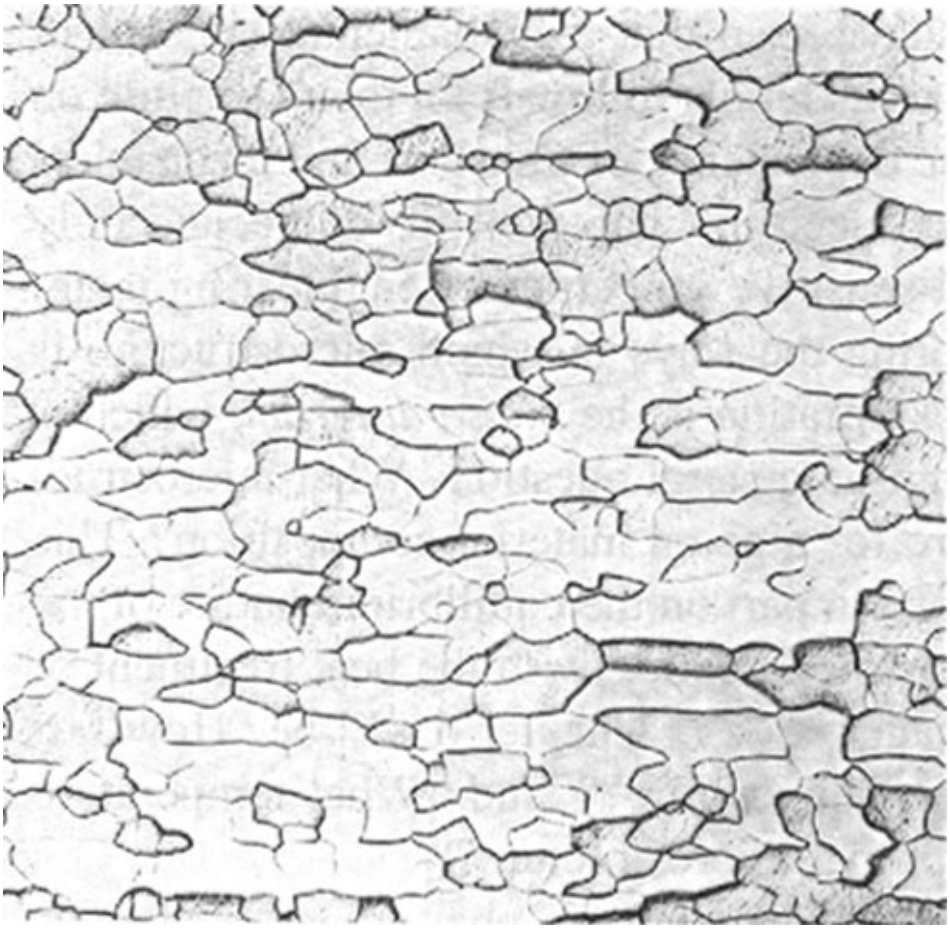

Figure 9-1 *Single-phase microstructure of commercially pure molybdenum, 200×. Although there are many grains in this microstructure, each grain has the same, uniform composition. (From* Metals Handbook, *8th ed., Vol. 7:* Atlas of Microstructures, *American Society for Metals, Metals Park, Ohio, 1972.)*

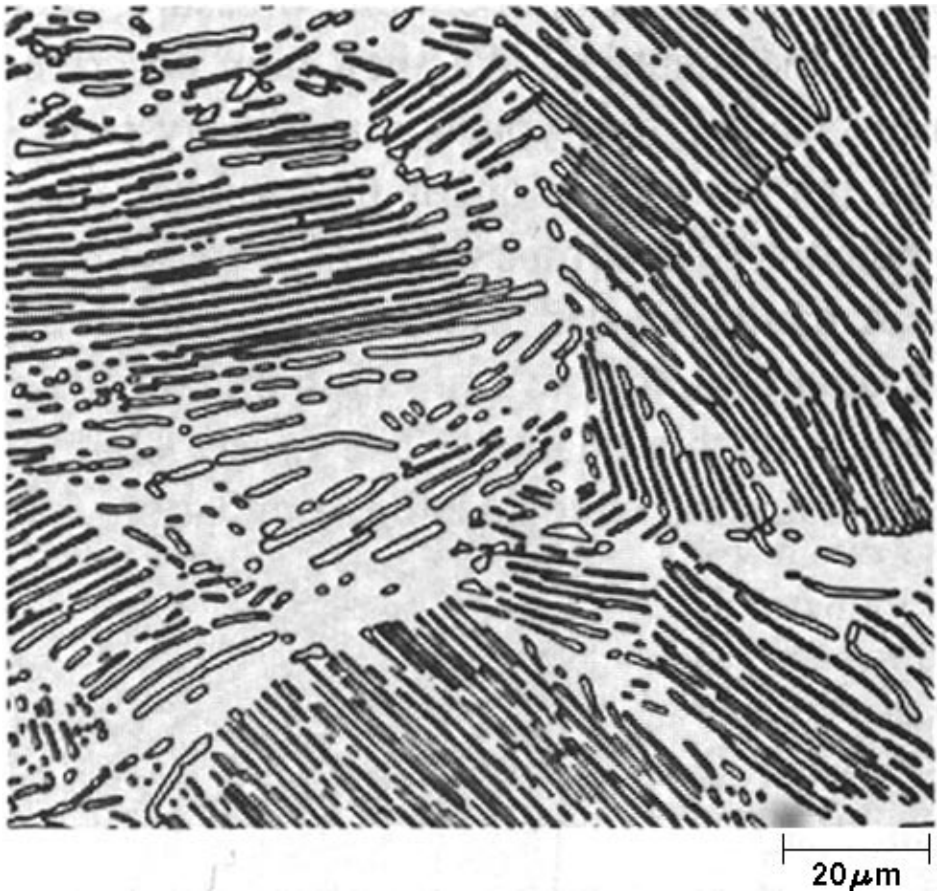

Figure 9-2 *Two-phase microstructure of pearlite found in a steel with 0.8 wt % C,* 500×. *This carbon content is an average of the carbon content in each of the alternating layers of ferrite (with <0.02 wt % C) and cementite (a compound, Fe_3C, which contains 6.7 wt % C). The narrower layers are the cementite phase. (From* Metals Handbook, *9th ed., Vol. 9:* Metallography and Microstructures, *American Society for Metals, Metals Park, Ohio, 1985.)*

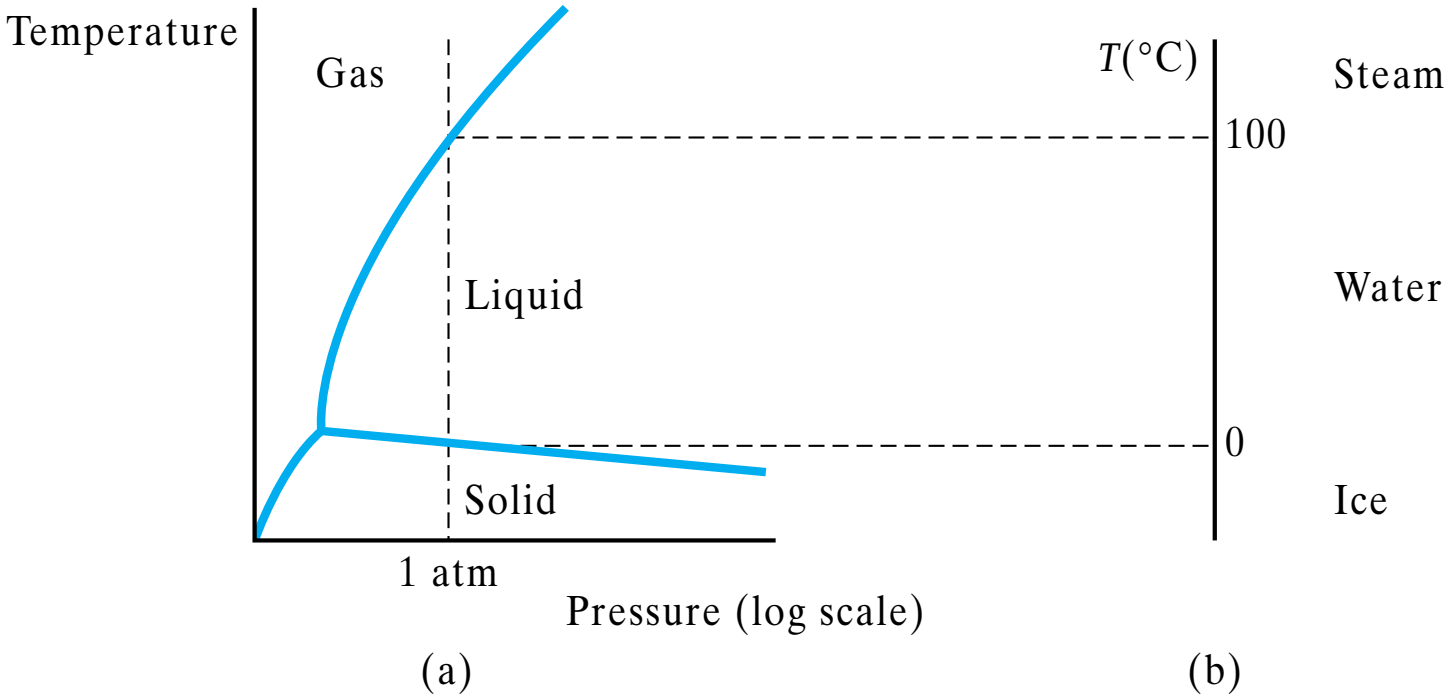

Figure 9-3 *(a) Schematic representation of the one-component phase diagram for H_2O. (b) A projection of the phase diagram information at 1 atm generates a temperature scale labeled with the familiar transformation temperatures for H_2O (melting at 0°C and boiling at 100°C).*

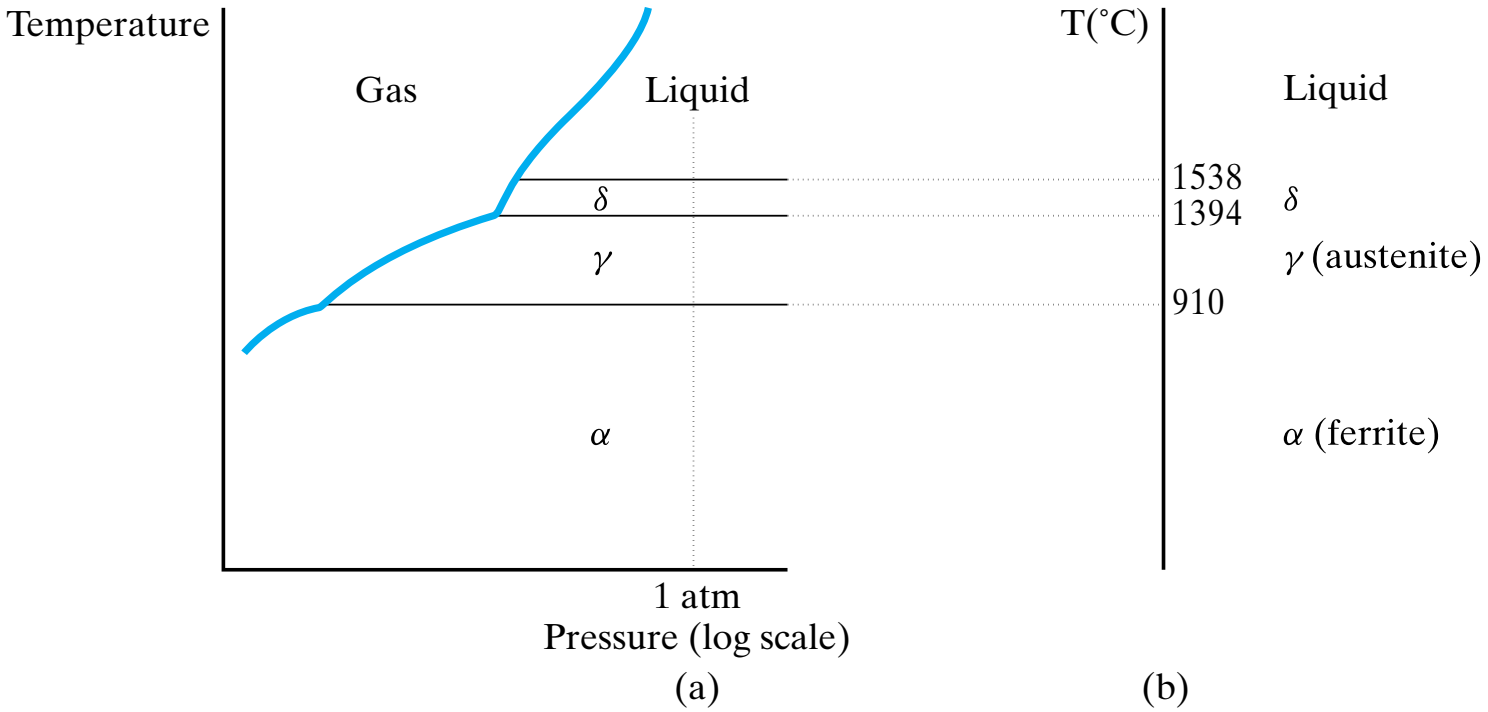

Figure 9-4 *(a) Schematic representation of the one-component phase diagram for pure iron. (b) A projection of the phase diagram information at 1 atm generates a temperature scale labeled with important transformation temperatures for iron. This projection will become one end of important binary diagrams such as Figure 9–19.*

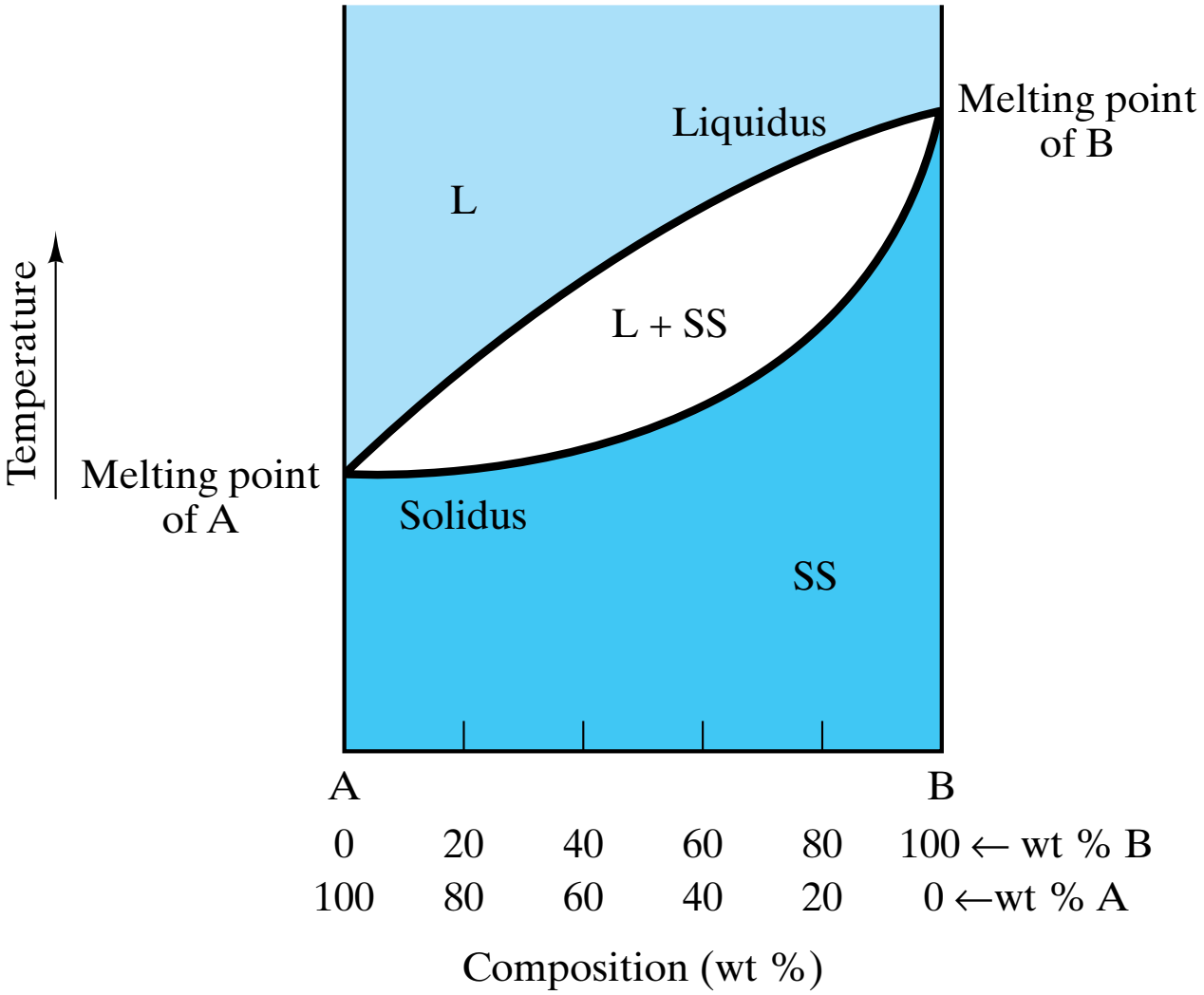

Figure 9-5 *Binary phase diagram showing complete solid solution. The liquid-phase field is labeled L and the solid solution is designated SS. Note the two-phase region labeled L + SS.*

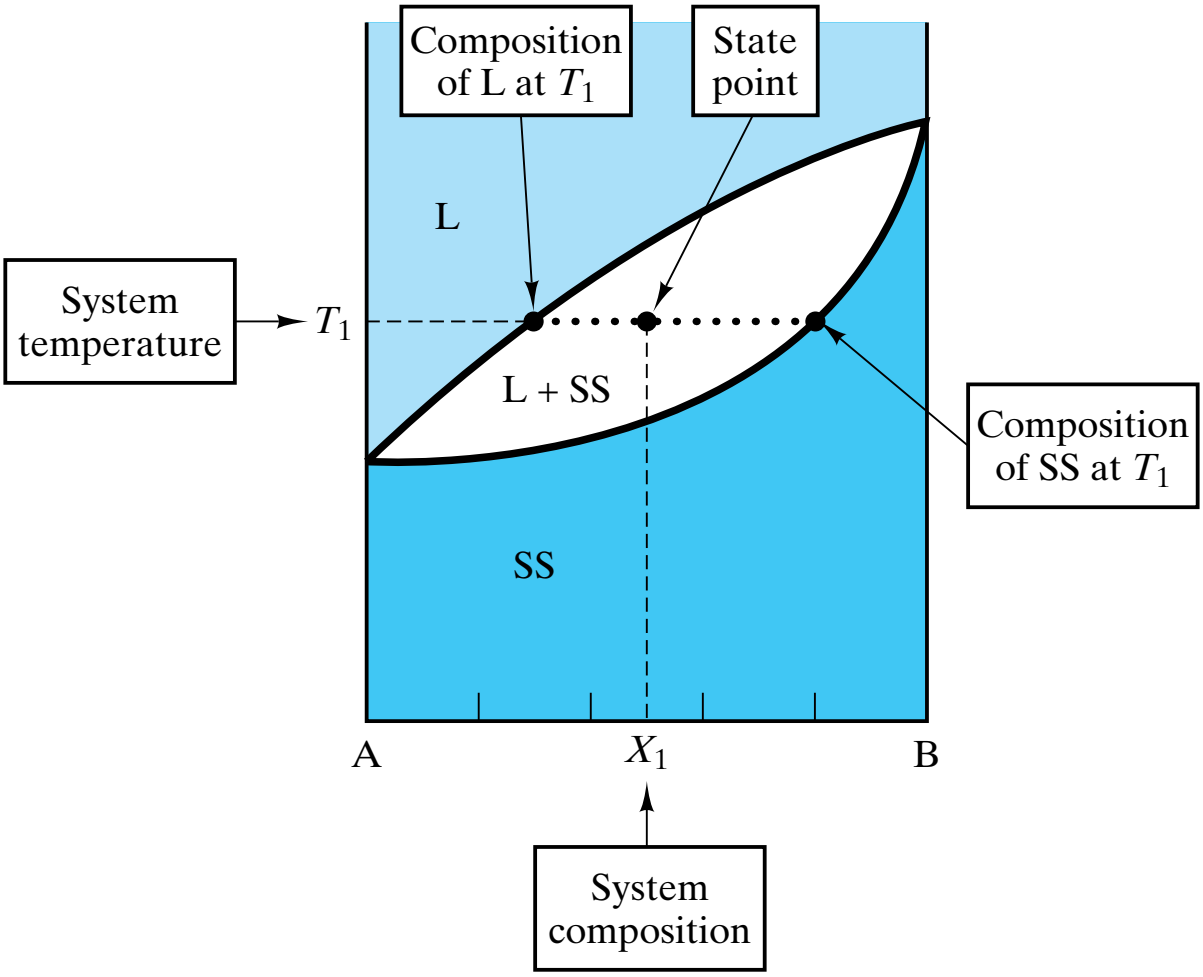

Figure 9-6 *The compositions of the phases in a two-phase region of the phase diagram are determined by a tie line (the horizontal line connecting the phase compositions at the system temperature).*

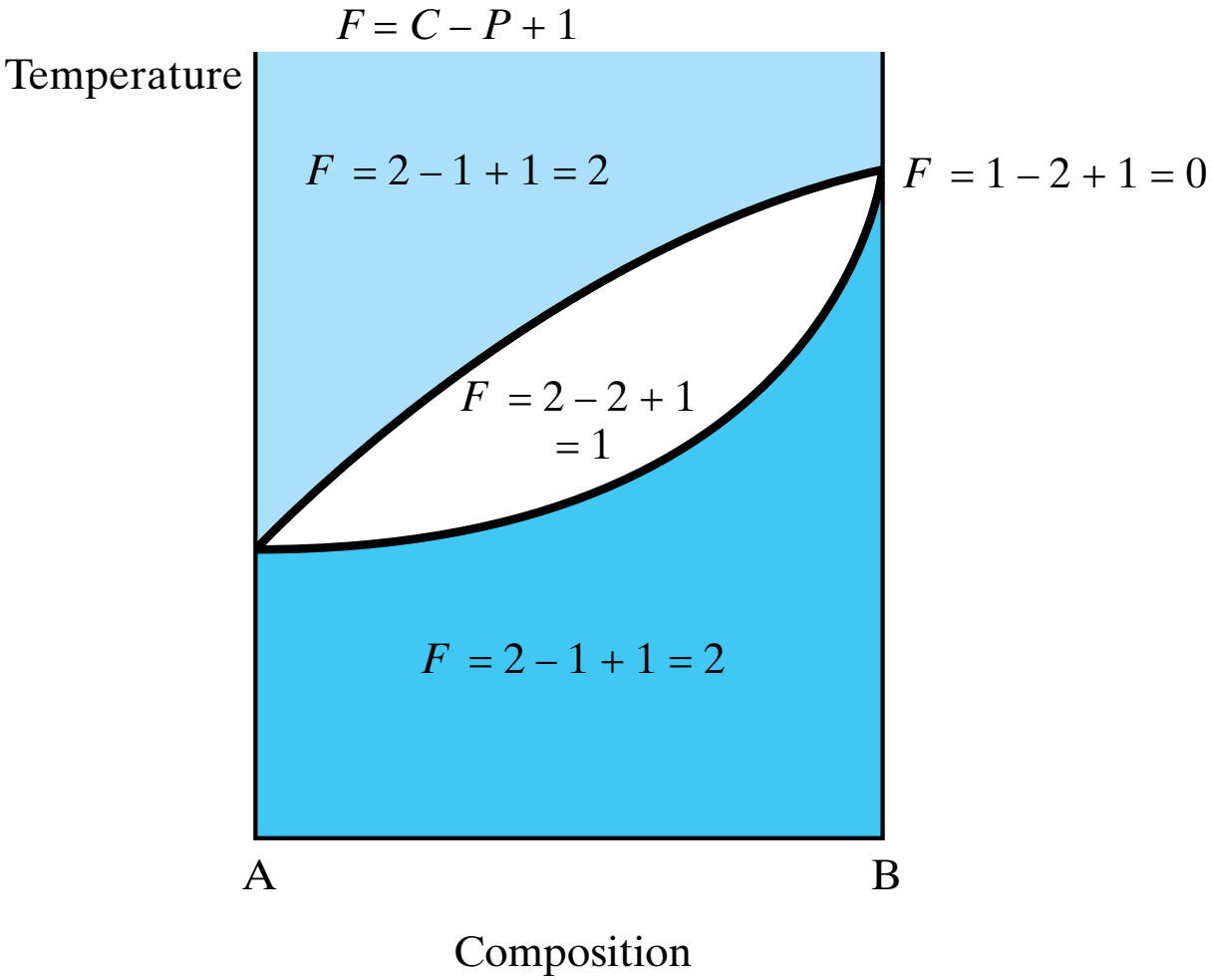

Figure 9-7 *Application of Gibbs phase rule (Equation 9.2) to various points in the phase diagram of Figure 9–5.*

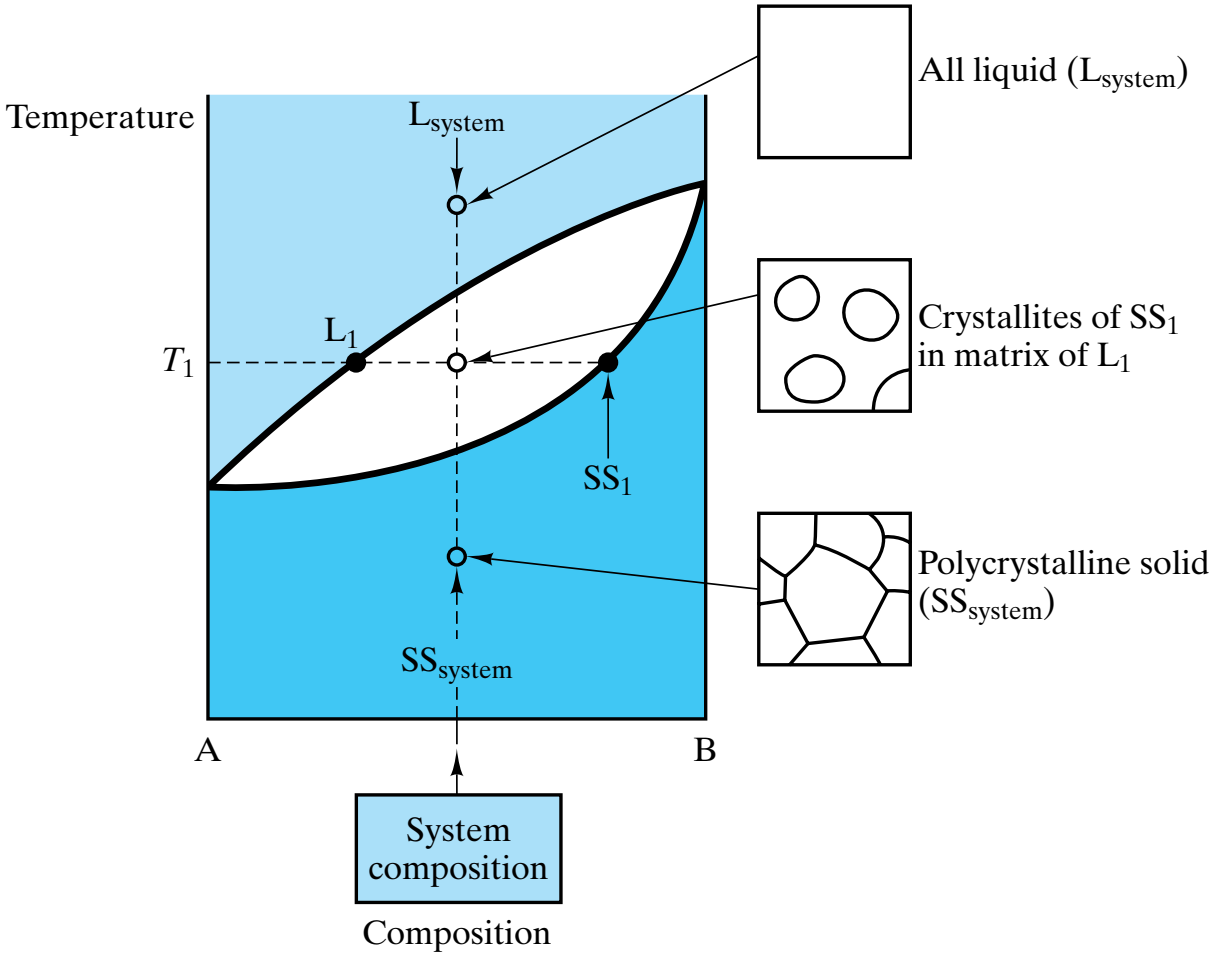

Figure 9-8 *Various microstructures characteristic of different regions in the complete solid-solution phase diagram.*

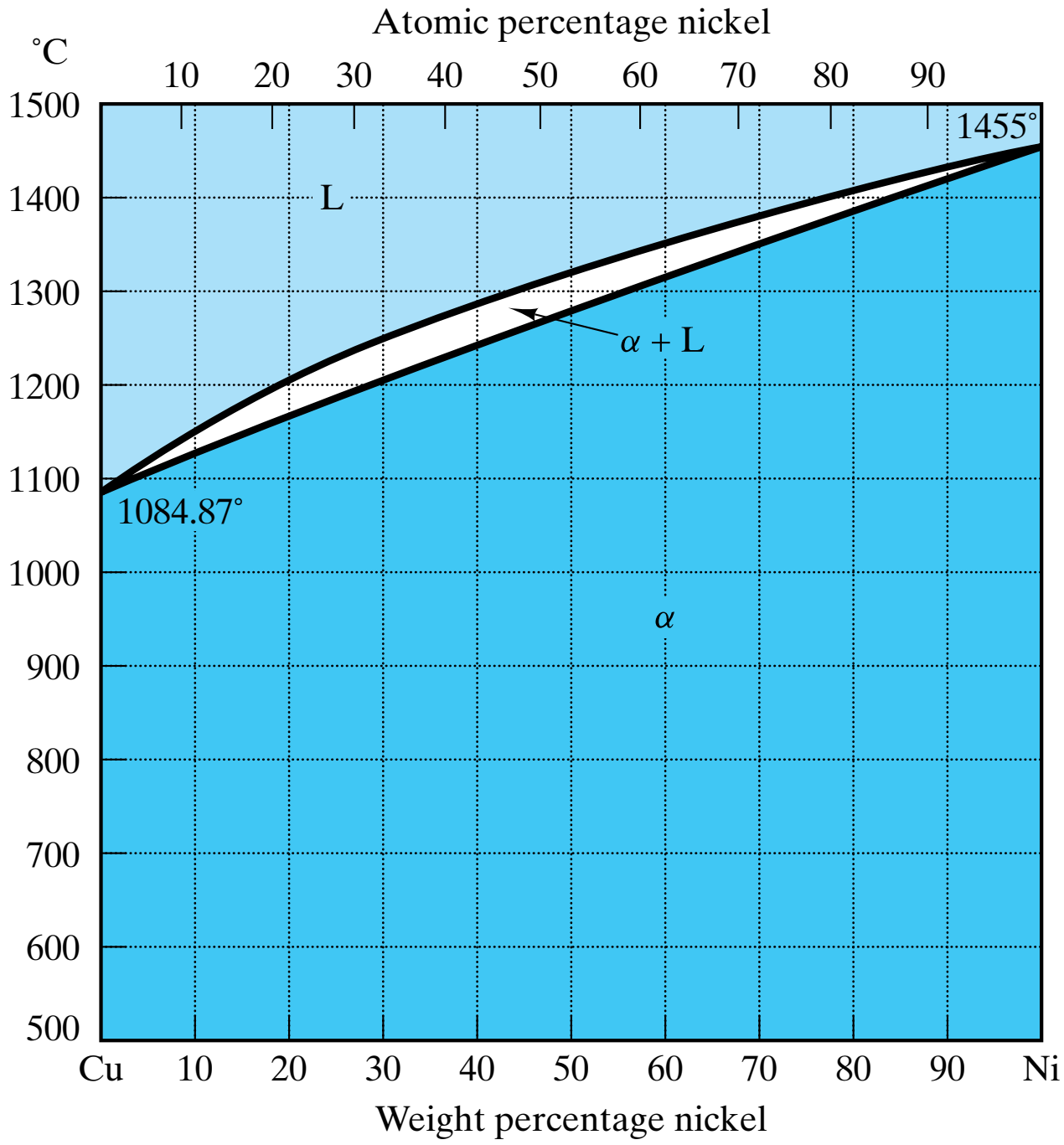

Figure 9-9 *Cu–Ni phase diagram. (After* Metals Handbook, *8th ed., Vol. 8:* Metallography, Structures, and Phase Diagrams, *American Society for Metals, Metals Park, Ohio, 1973, and* Binary Alloy Phase Diagrams, *Vol. 1, T. B. Massalski, ed., American Society for Metals, Metals Park, Ohio, 1986.)*

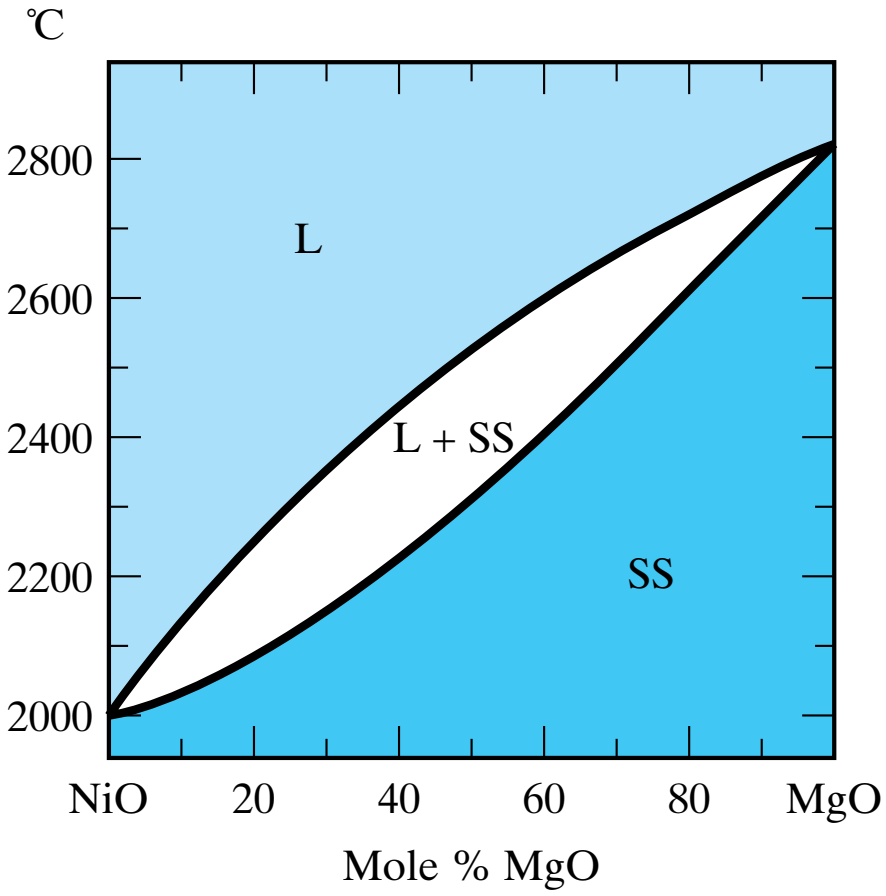

Figure 9-10 *NiO–MgO phase diagram. (After* Phase Diagrams for Ceramists, *Vol. 1, American Ceramic Society, Columbus, Ohio, 1964.)*

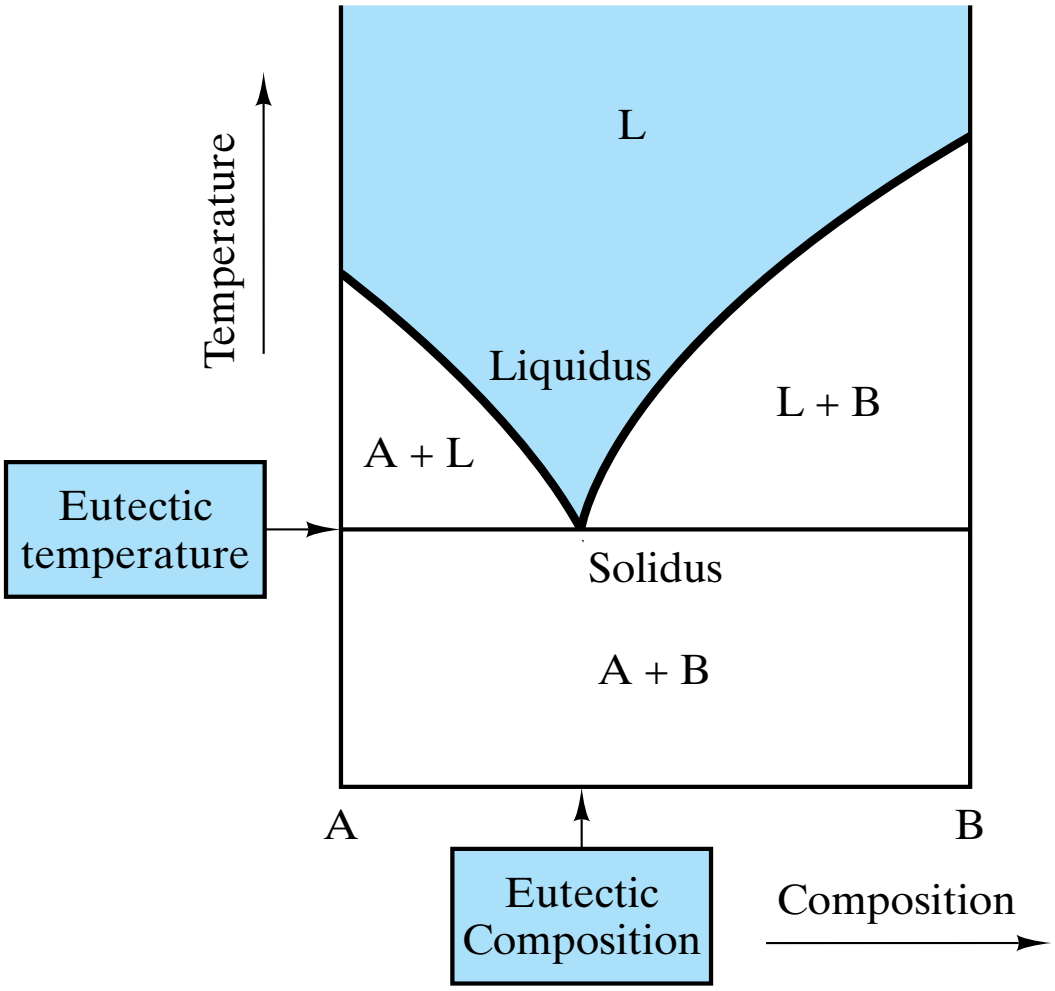

Figure 9-11 *Binary eutectic phase diagram showing no solid solution. This general appearance can be contrasted to the opposite case of complete solid solution illustrated in Figure 9–5.*

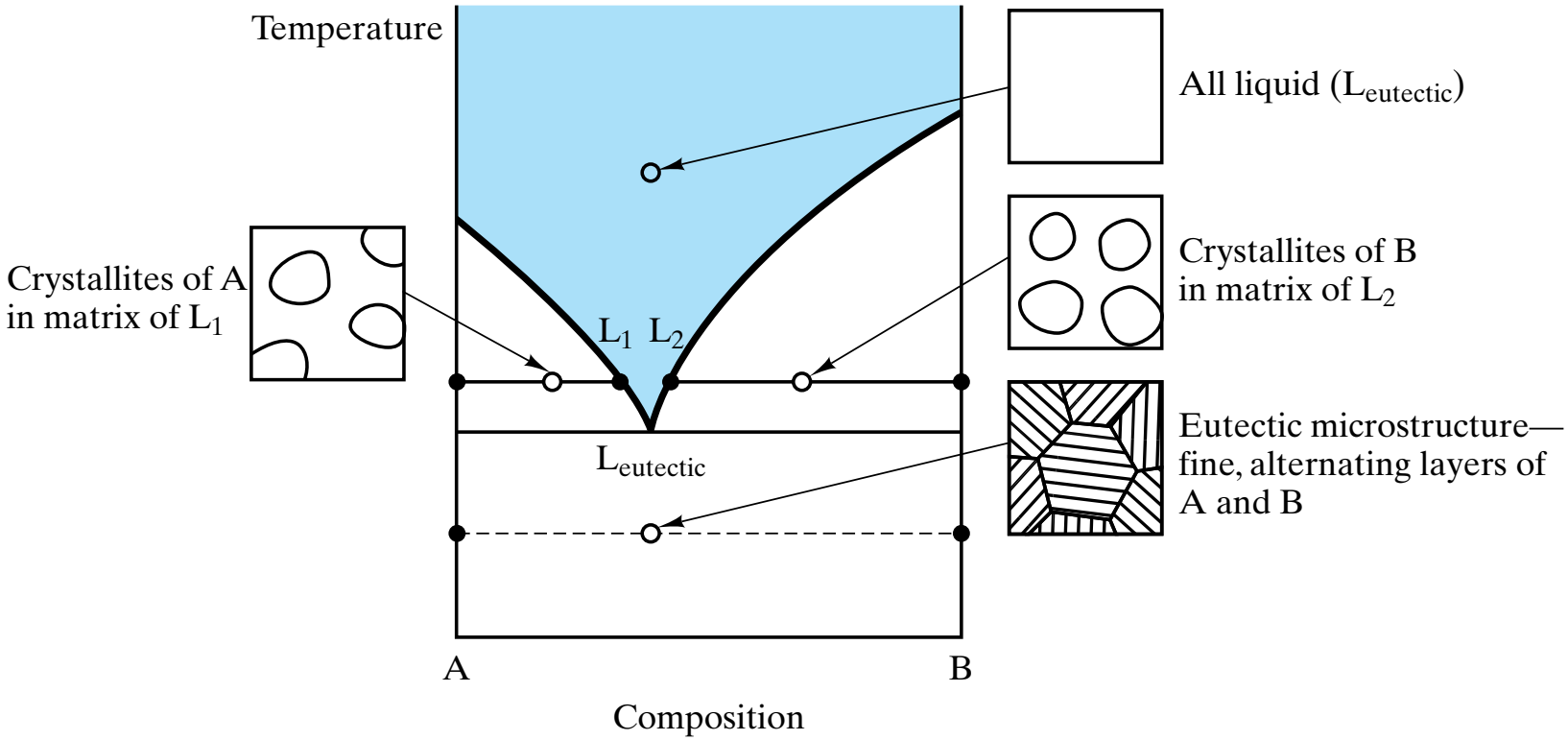

Figure 9-12 *Various microstructures characteristic of different regions in a binary eutectic phase diagram with no solid solution.*

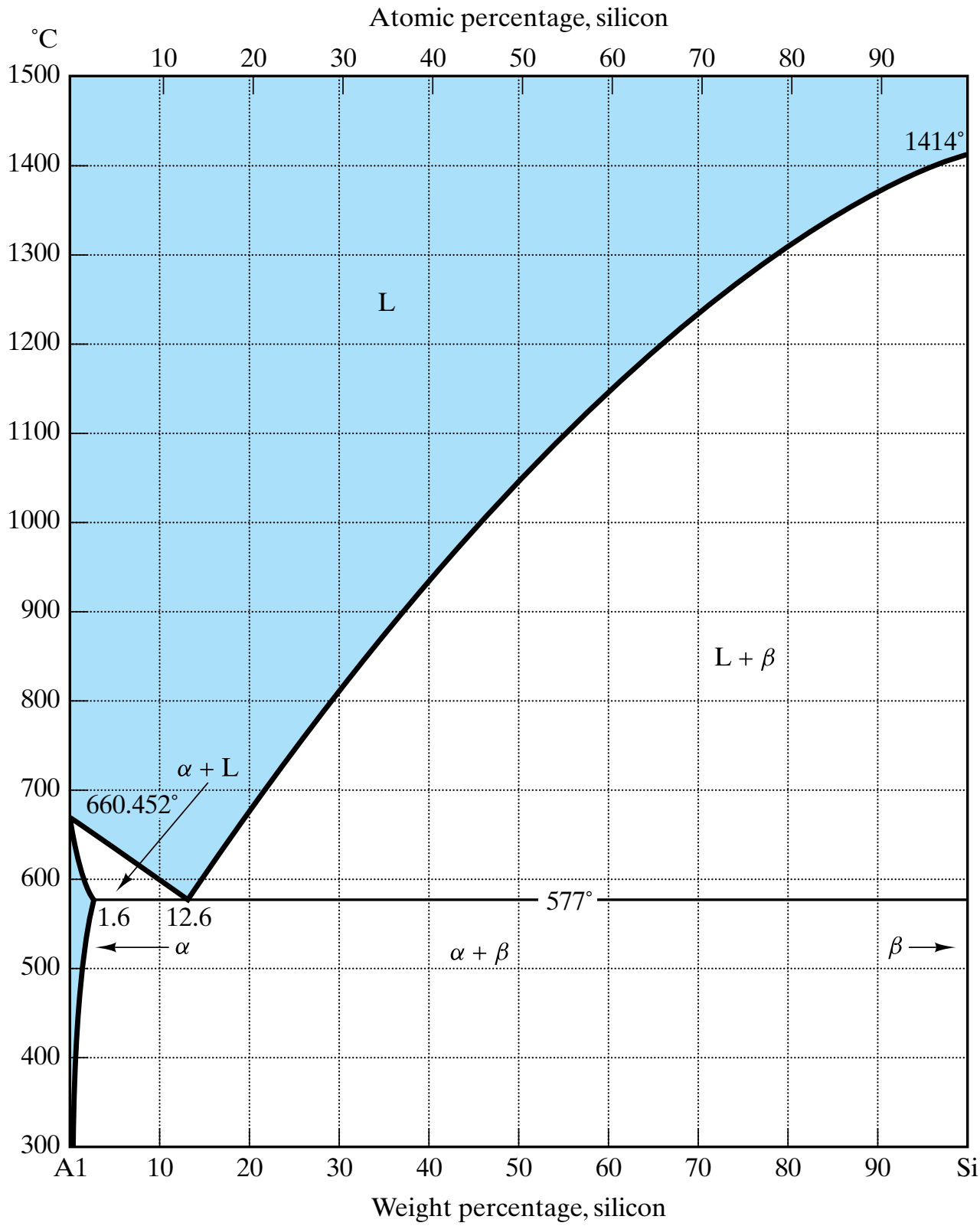

Figure 9-13 *Al–Si phase diagram. (After* Binary Alloy Phase Diagrams, *Vol. 1, T. B. Massalski, ed., American Society for Metals, Metals Park, Ohio, 1986.)*

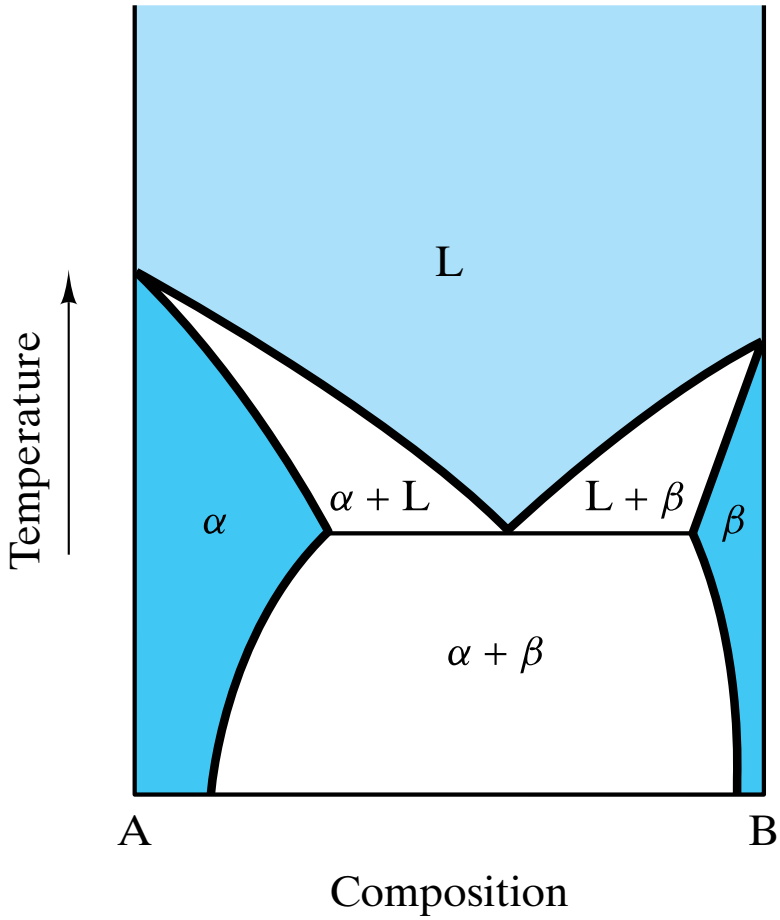

Figure 9-14 *Binary eutectic phase diagram with limited solid solution. The only difference from Figure 9–11 is the presence of solid-solution regions α and β.*

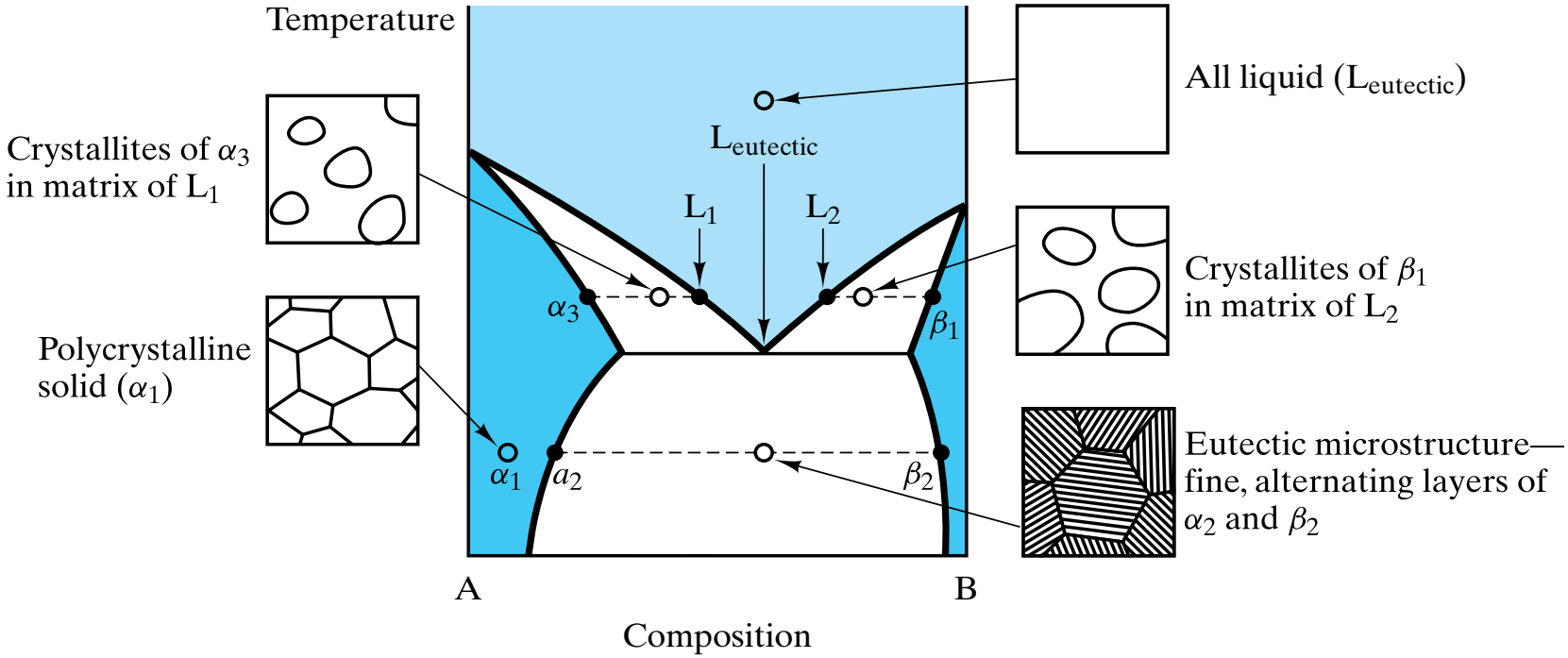

Figure 9-15 *Various microstructures characteristic of different regions in the binary eutectic phase diagram with limited solid solution. This illustration is essentially equivalent to Figure 9–12 except that the solid phases are now solid solutions (α and β) rather than pure components (A and B).*

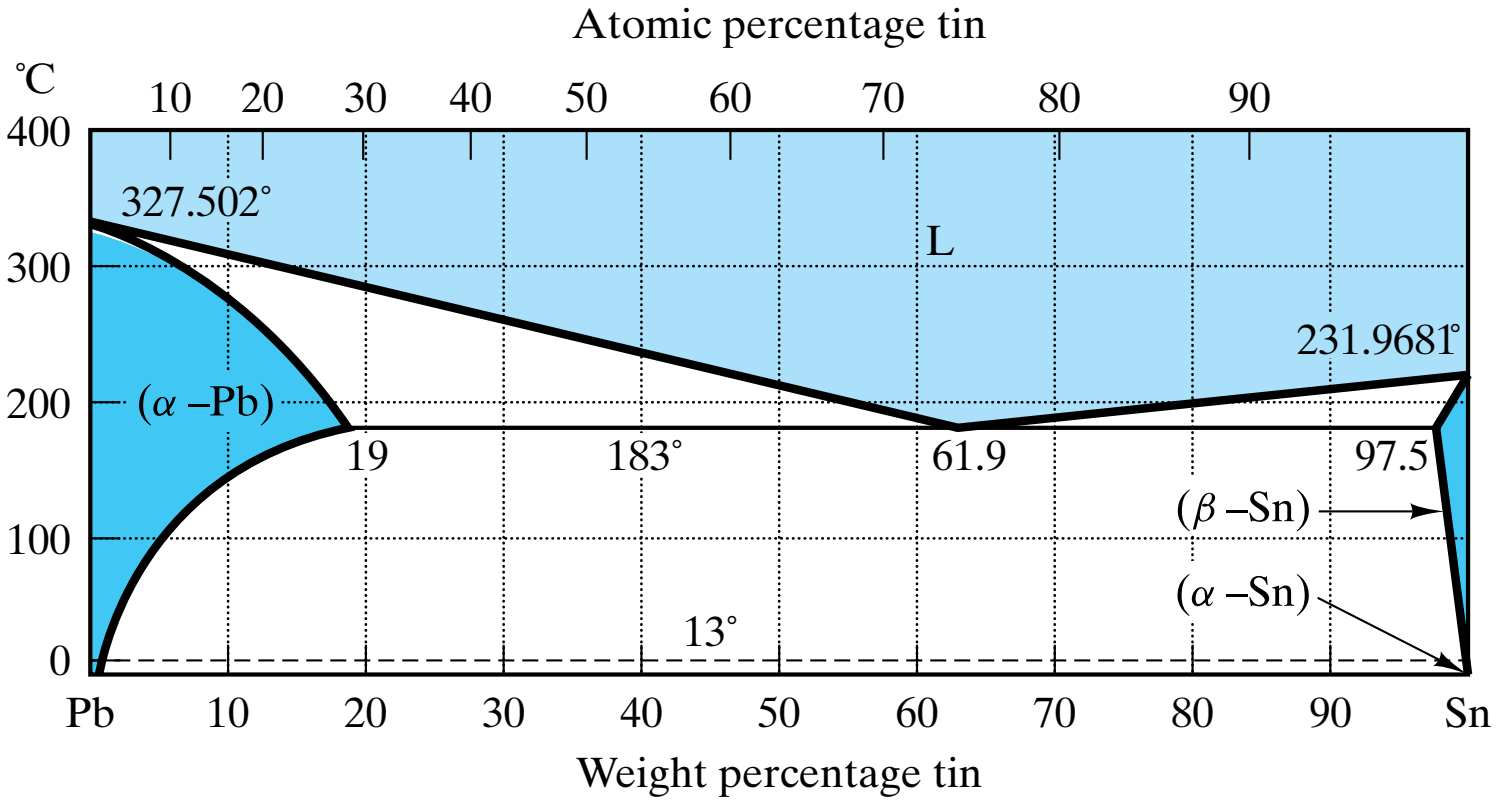

Figure 9-16 *Pb–Sn phase diagram. (After* Metals Handbook, *8th ed., Vol. 8:* Metallography, Structures, and Phase Diagrams, *American Society for Metals, Metals Park, Ohio, 1973, and* Binary Alloy Phase Diagrams, *Vol. 2, T. B. Massalski, ed., American Society for Metals, Metals Park, Ohio, 1986.)*

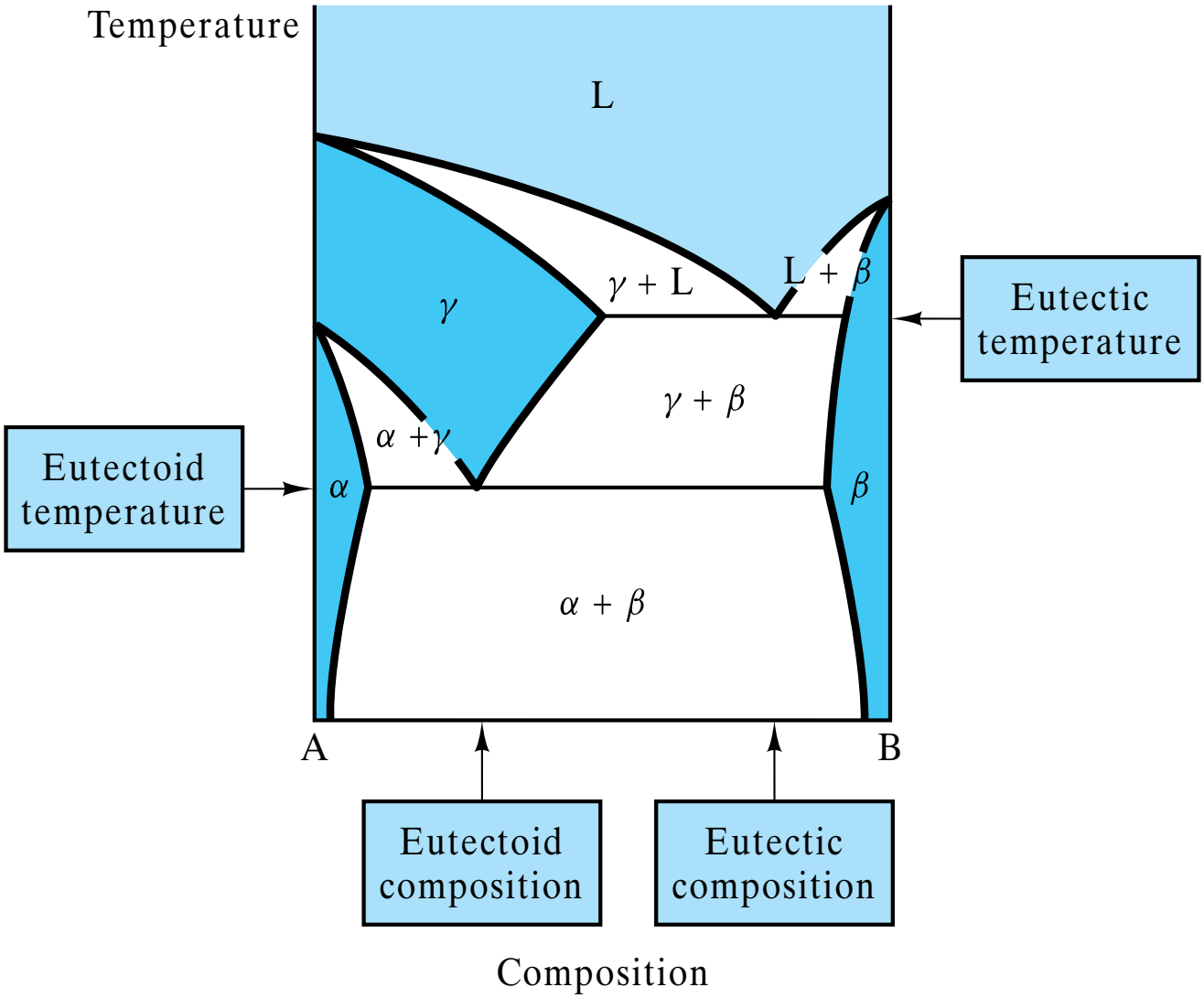

Figure 9-17 *This eutectoid phase diagram contains both a eutectic reaction (Equation 9.3) and its solid-state analog, a eutectoid reaction (Equation 9.4).*

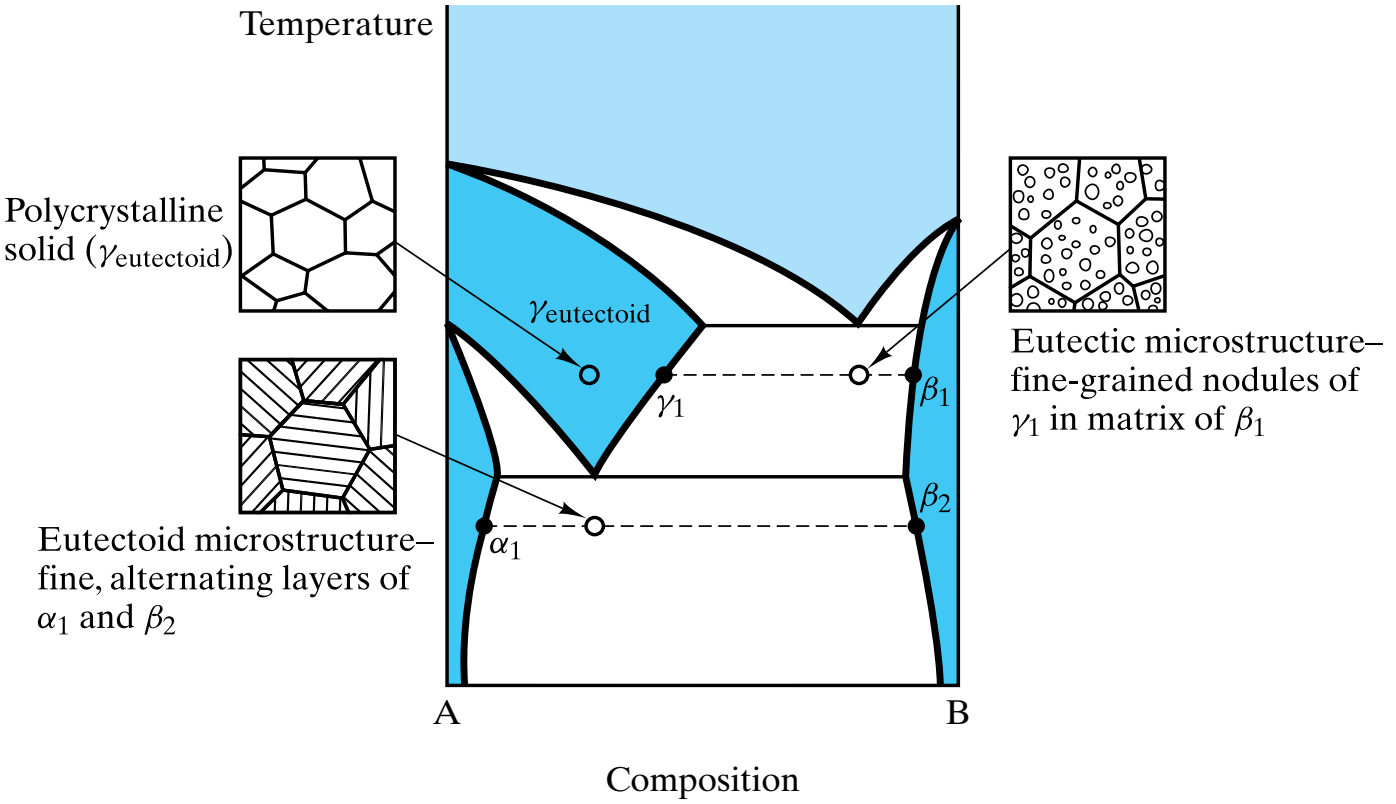

Figure 9-18 *Representative microstructures for the eutectoid diagram of Figure 9–17.*

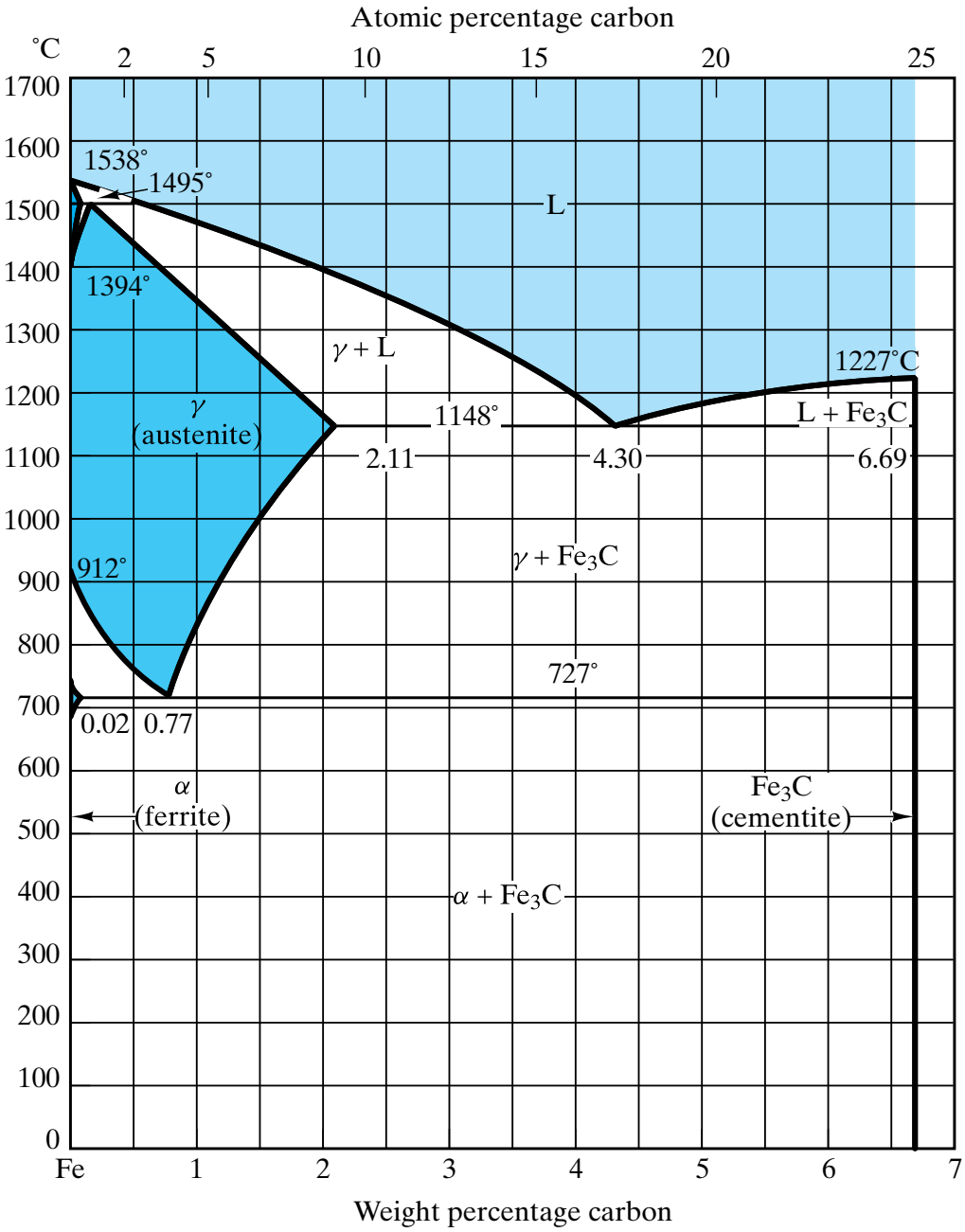

Figure 9-19 *Fe–Fe_3C phase diagram. Note that the composition axis is given in weight percent carbon even though Fe_3C, and not carbon, is a component. (After* Metals Handbook, *8th ed., Vol. 8:* Metallography, Structures, and Phase Diagrams, *American Society for Metals, Metals Park, Ohio, 1973, and* Binary Alloy Phase Diagrams, *Vol. 1, T. B. Massalski, ed., American Society for Metals, Metals Park, Ohio, 1986.)*

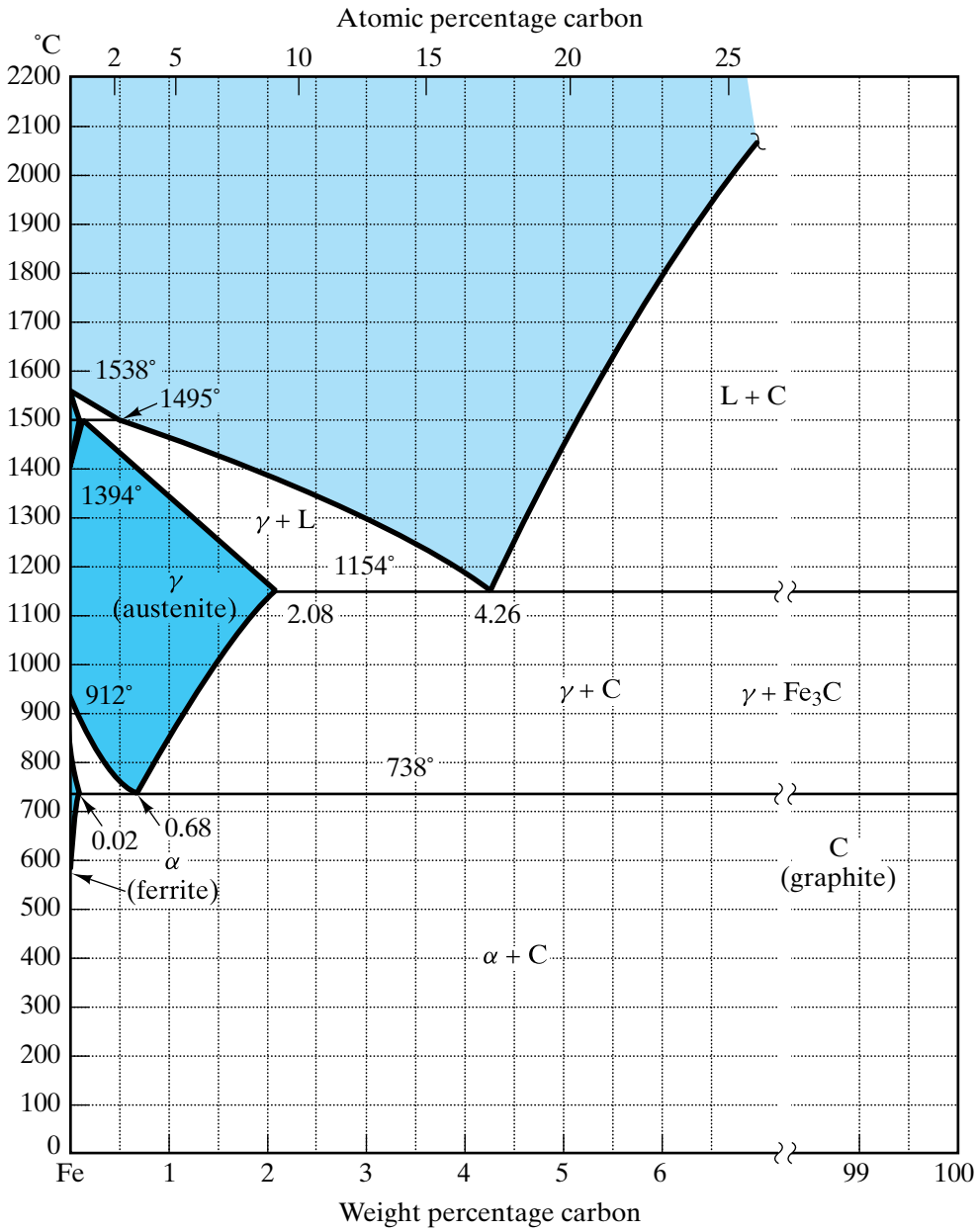

Figure 9-20 *Fe–C phase diagram. The left side of this diagram is nearly identical to that for the Fe–Fe_3C diagram (Figure 9–19). In this case, however, the intermediate compound Fe_3C does not exist. (After* Metals Handbook, *8th ed., Vol. 8:* Metallography, Structures, and Phase Diagrams, *American Society for Metals, Metals Park, Ohio, 1973, and* Binary Alloy Phase Diagrams, *Vol. 1, T. B. Massalski, ed., American Society for Metals, Metals Park, Ohio, 1986.)*

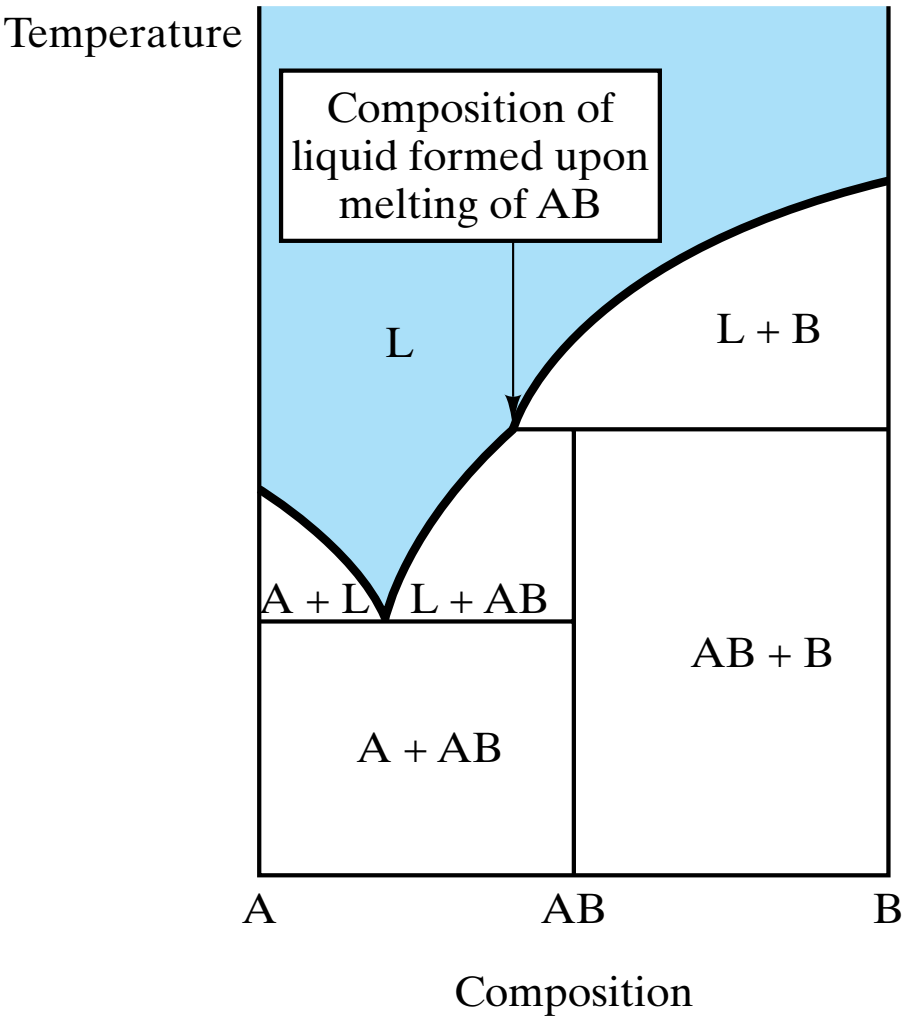

Figure 9-21 *Peritectic phase diagram showing a peritectic reaction (Equation 9.5). For simplicity, no solid solution is shown.*

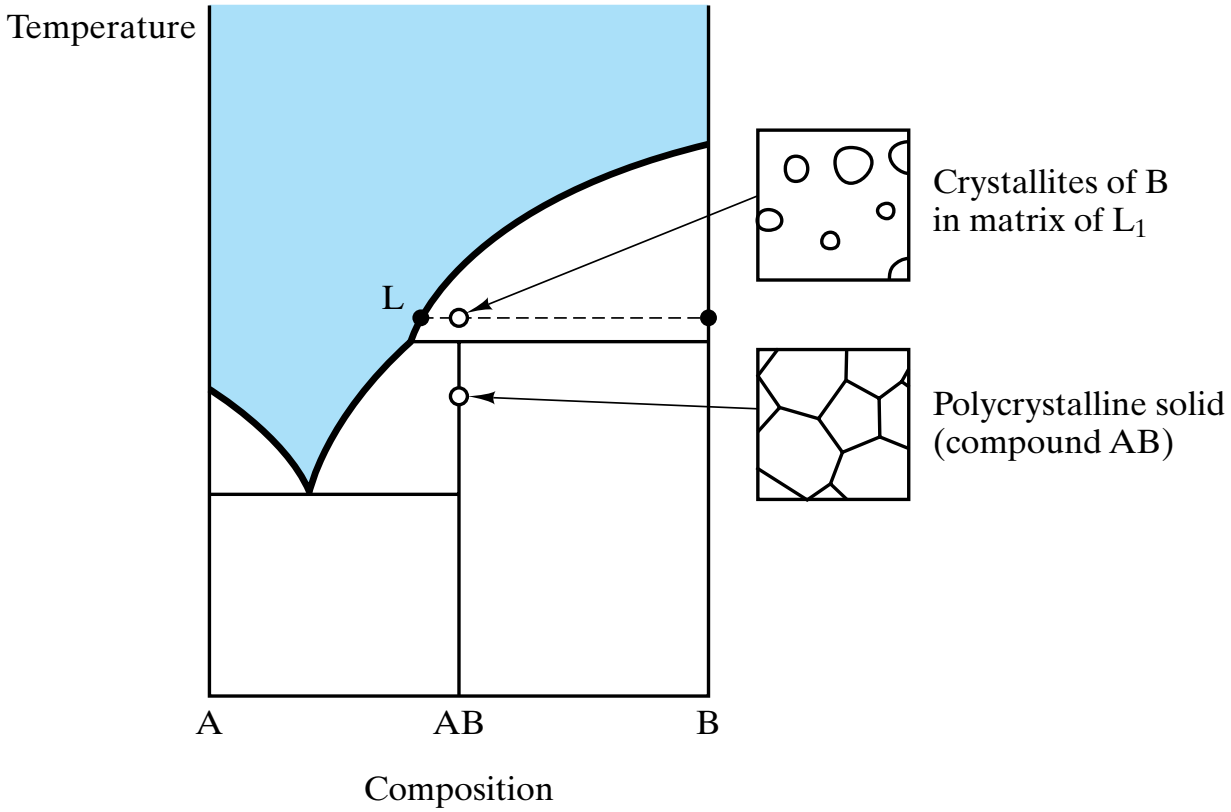

Figure 9-22 *Representative microstructures for the peritectic diagram of Figure 9–21.*

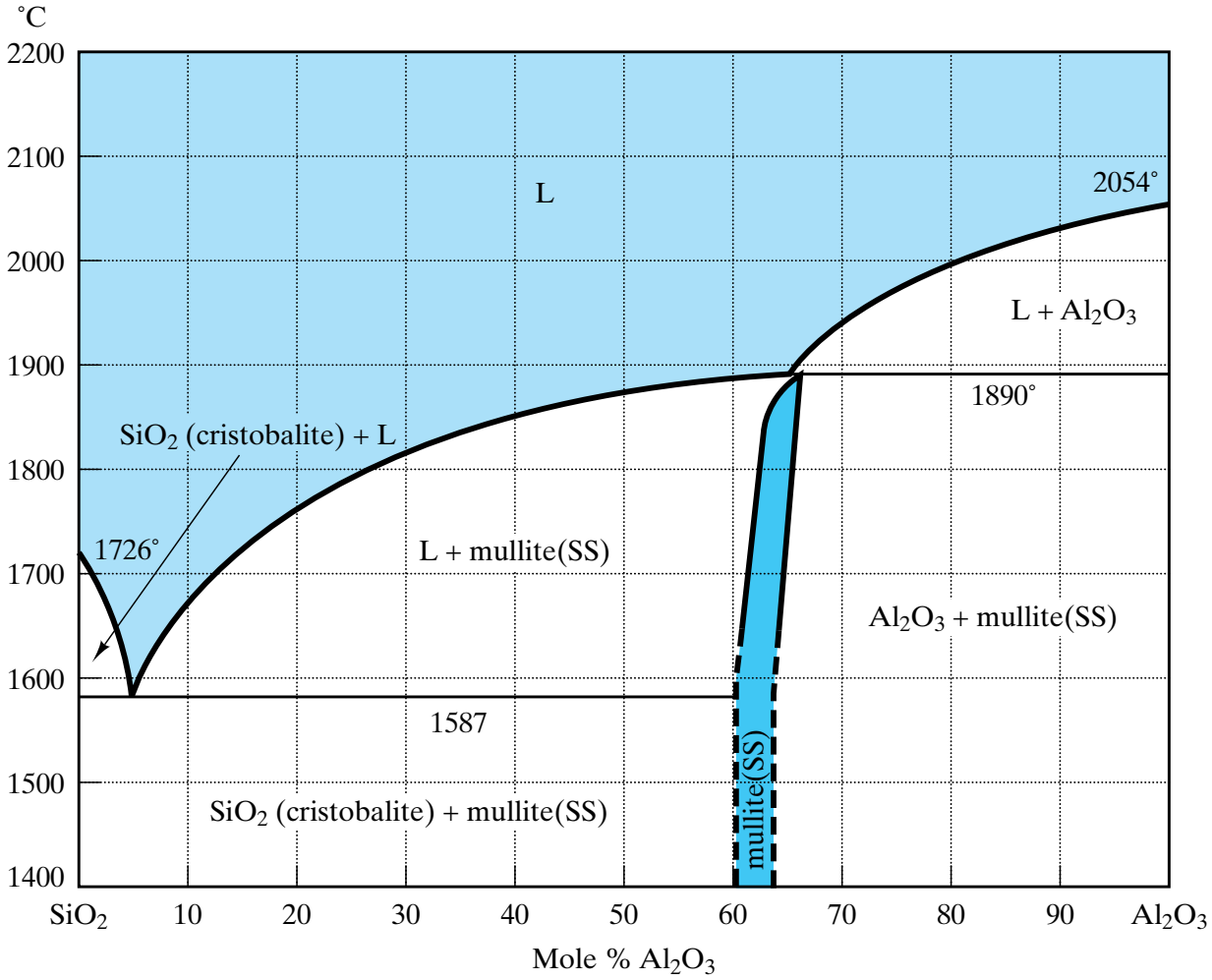

Figure 9-23 *Al_2O_3–SiO_2 phase diagram. Mullite is an intermediate compound with ideal stoichiometry $3Al_2O_3 \cdot 2SiO_2$. (After F. J. Klug, S. Prochazka, and R. H. Doremus,* J. Am. Ceram. Soc. 70, *750 (1987).)*

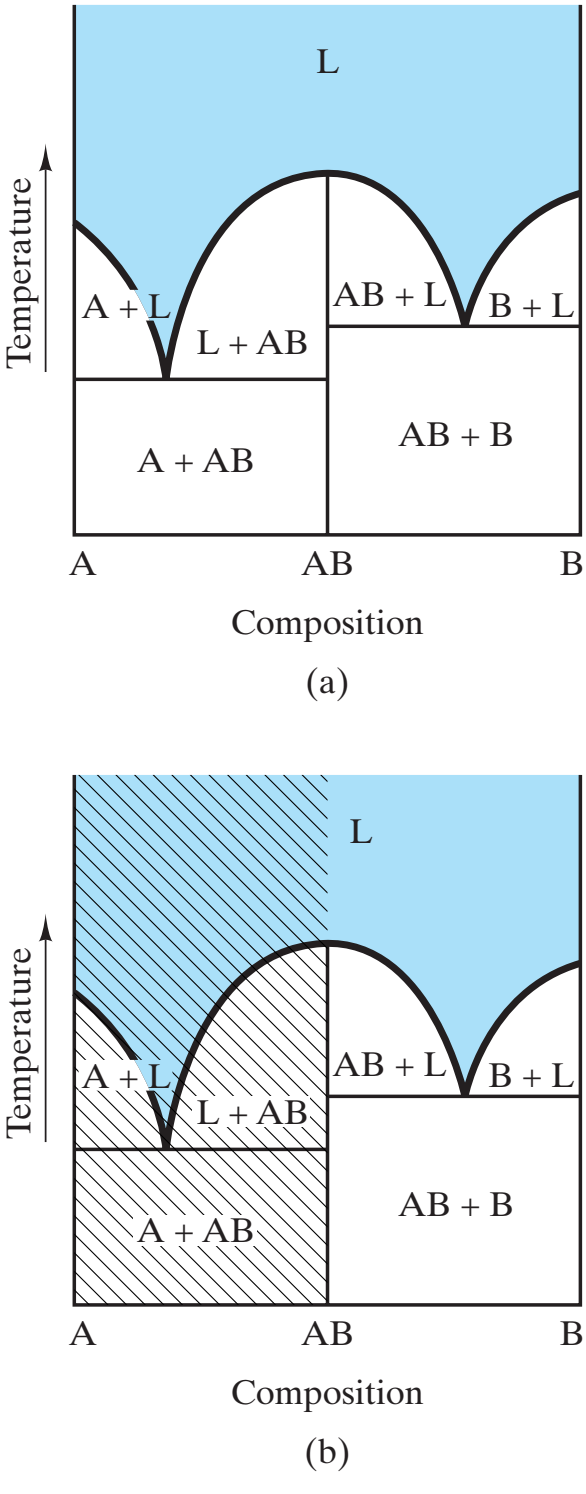

Figure 9-24 *(a) Binary phase diagram with a congruently melting intermediate compound, AB. This diagram is equivalent to two simple binary eutectic diagrams (the A–AB and AB–B systems). (b) For analysis of microstructure for an overall composition in the AB–B system, only that binary eutectic diagram need be considered.*

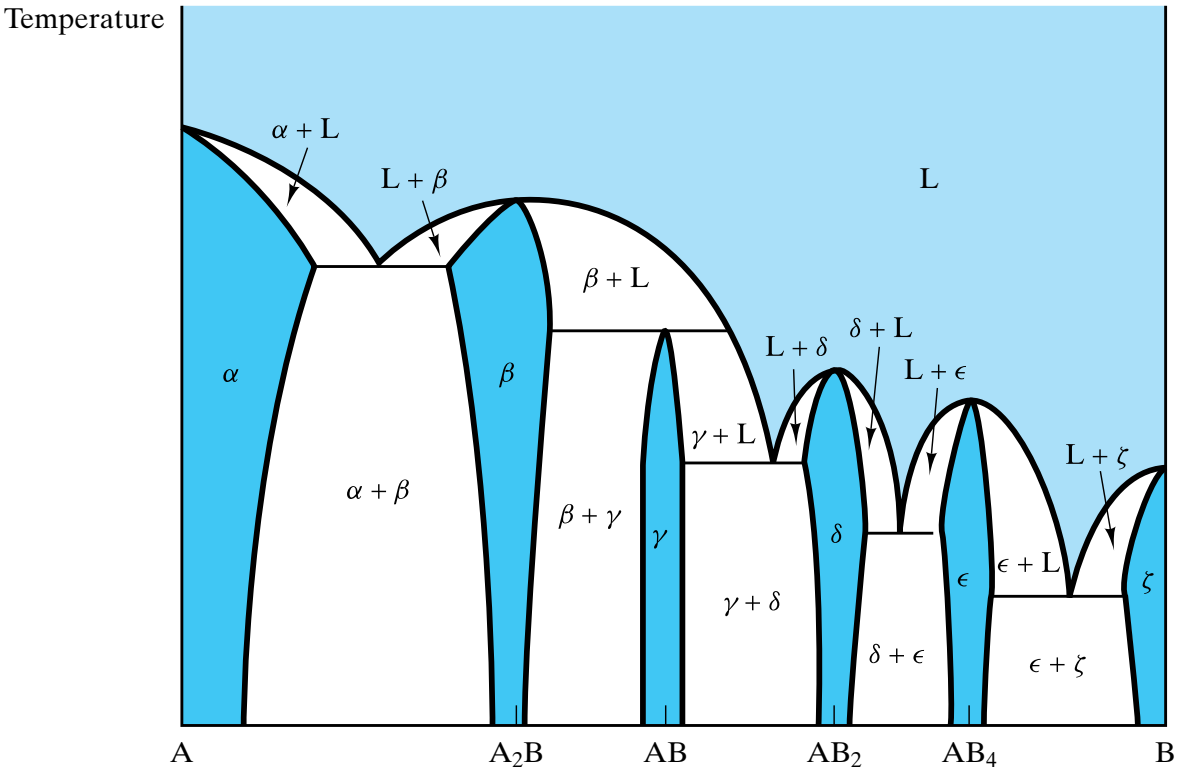
Temperature
α + L
L + β
L
β + L
L + δ
δ + L
L + ϵ
α
β
γ + L
L + ζ
α + β
β + γ
γ
δ
ϵ + L
ϵ
ζ
γ + δ
δ + ϵ
ϵ + ζ
A
A2B
AB
AB2
AB4
B
Composition

(a)

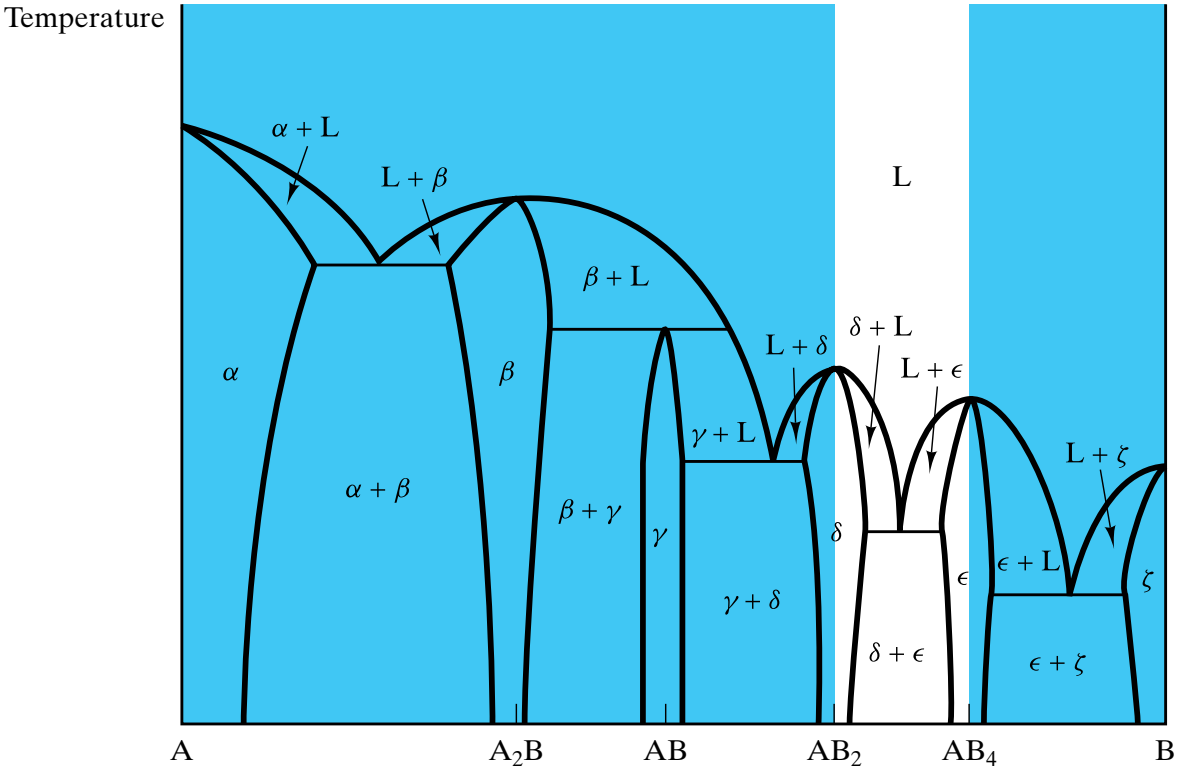
Temperature
α + L
L + β
L
β + L
L + δ
δ + L
L + ϵ
α
β
γ + L
L + ζ
α + β
β + γ
γ
δ
ϵ + L
ϵ
ζ
γ + δ
δ + ϵ
ϵ + ζ
A
A2B
AB
AB2
AB4
B
Composition

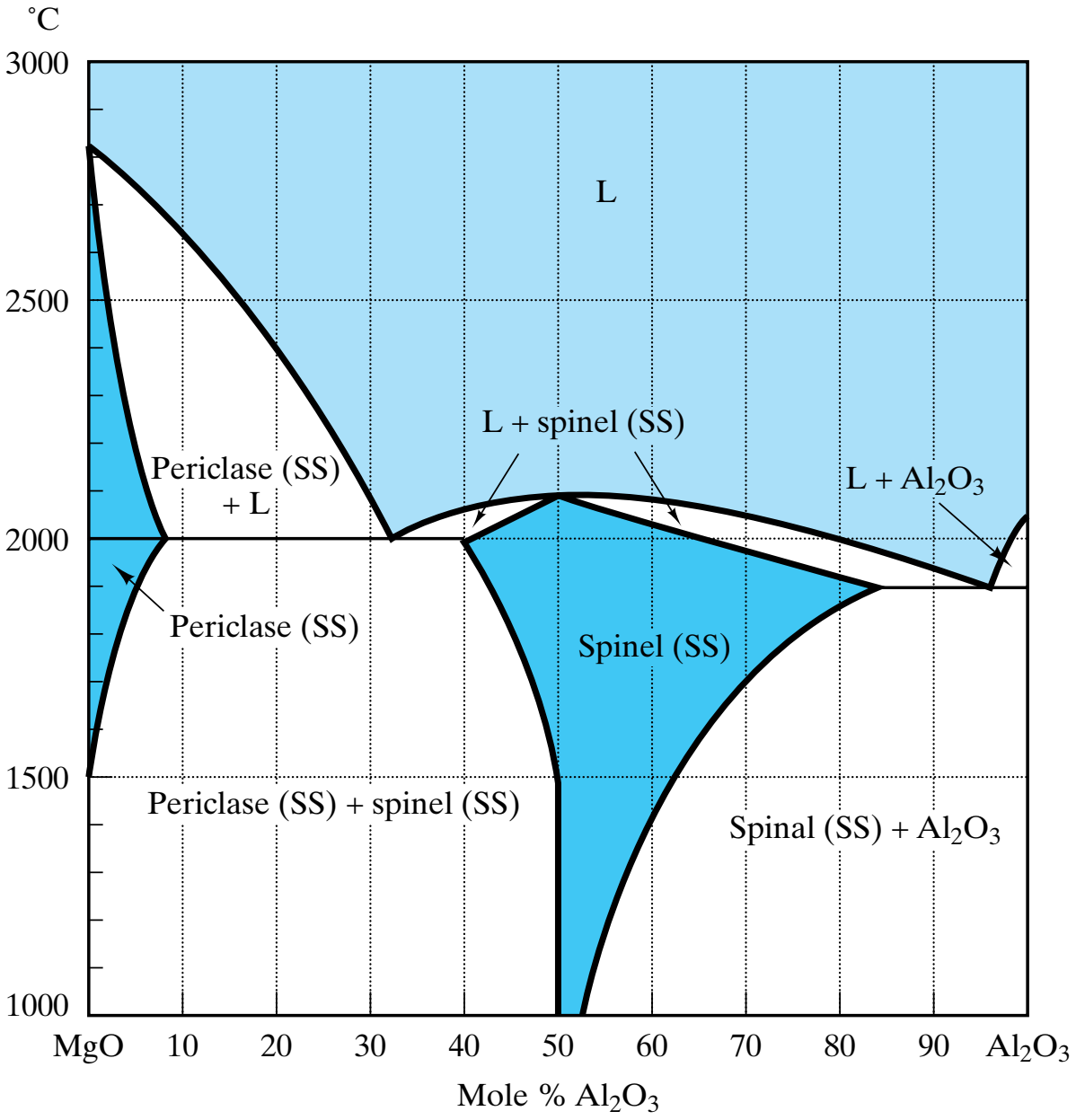

Figure 9-26 *MgO–Al_2O_3 phase diagram. Spinel is an intermediate compound with ideal stoichiometry $MgO \cdot Al_2O_3$. (After* Phase Diagrams for Ceramists, *Vol. 1, American Ceramic Society, Columbus, Ohio, 1964.)*

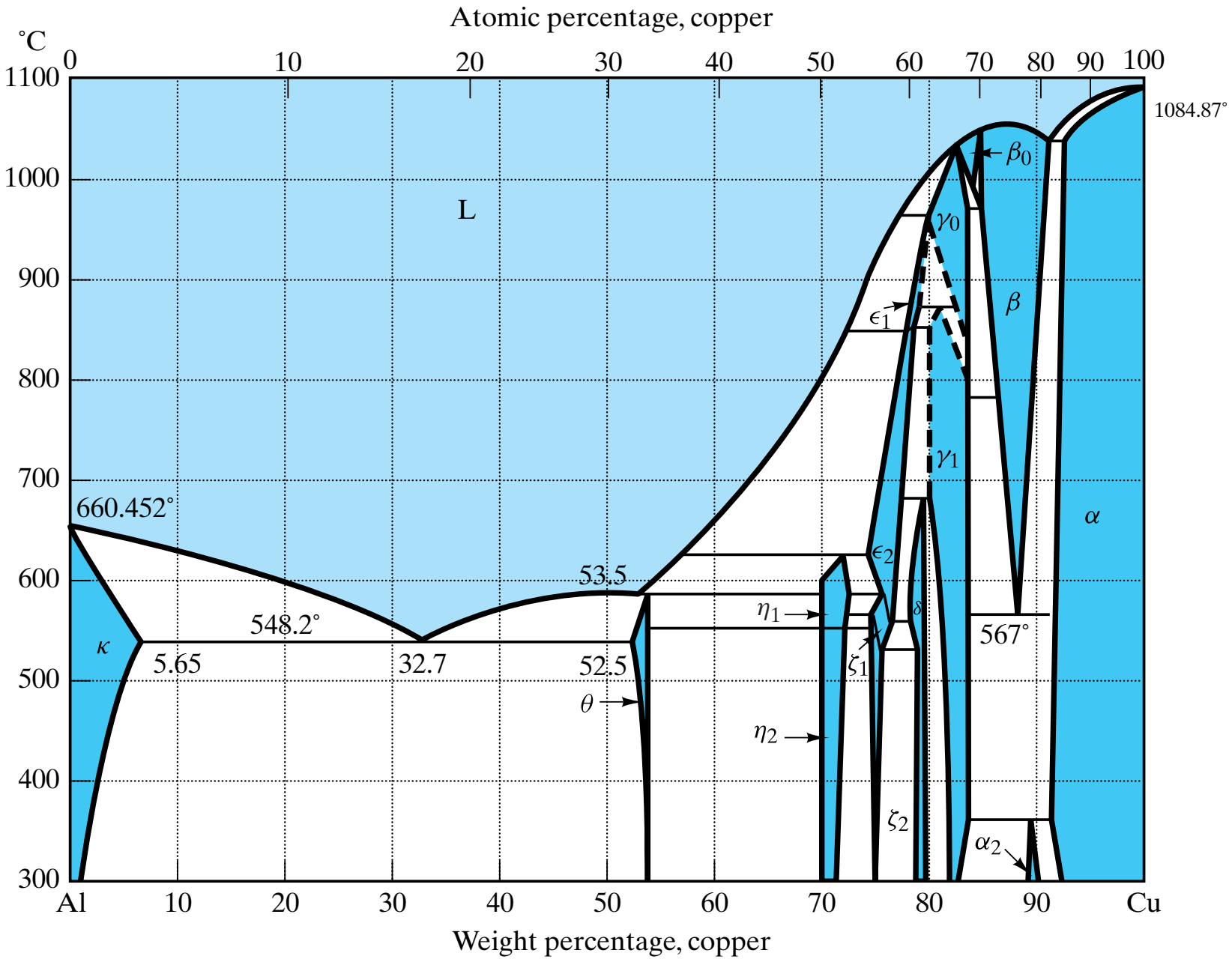

Figure 9-27 *Al–Cu phase diagram. (After* Binary Alloy Phase Diagrams, *Vol. 1, T. B. Massalski, ed., American Society for Metals, Metals Park, Ohio, 1986.)*

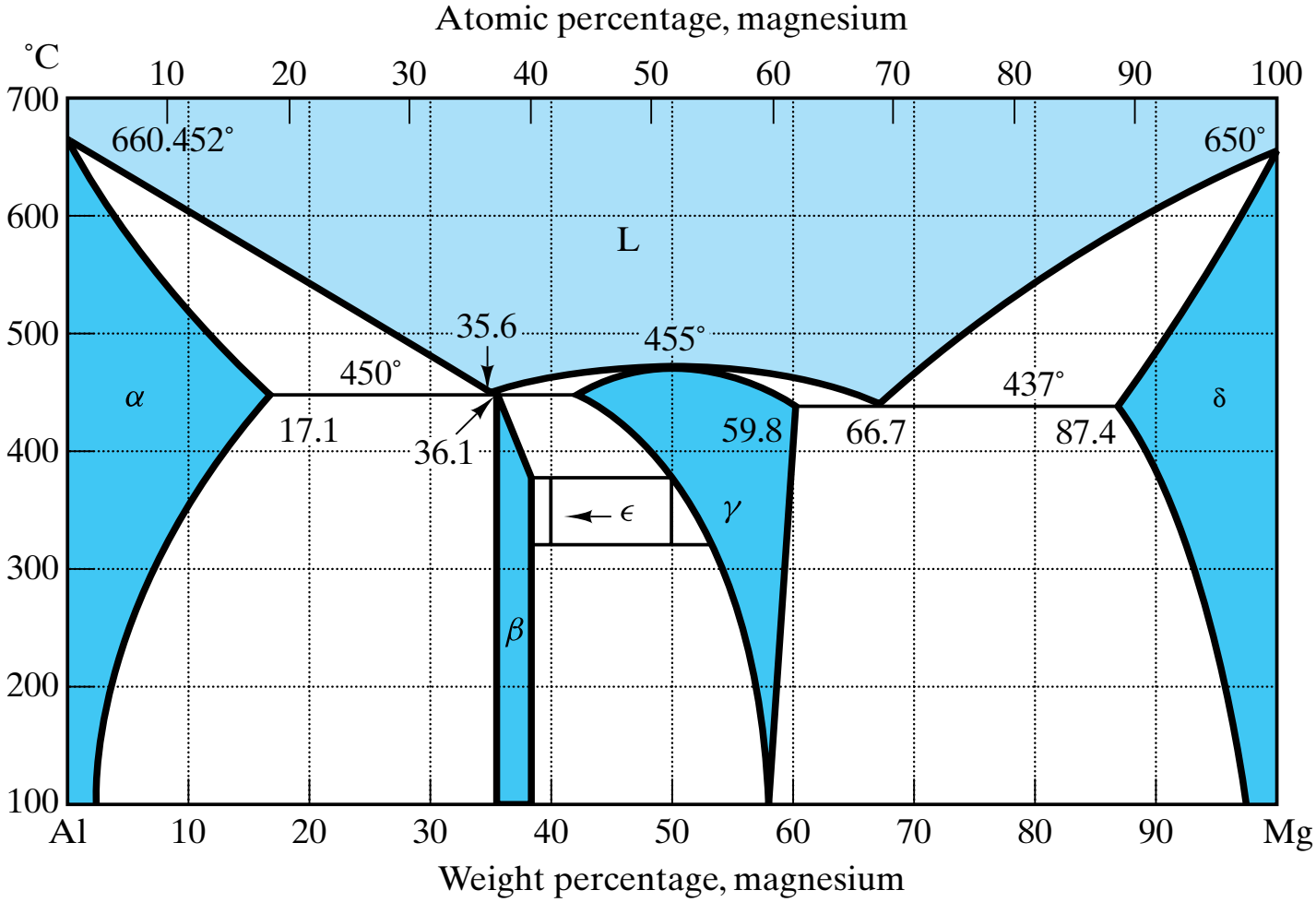

Figure 9-28 *Al–Mg phase diagram. (After* Binary Alloy Phase Diagrams, *Vol. 1, T. B. Massalski, ed., American Society for Metals, Metals Park, Ohio, 1986.)*

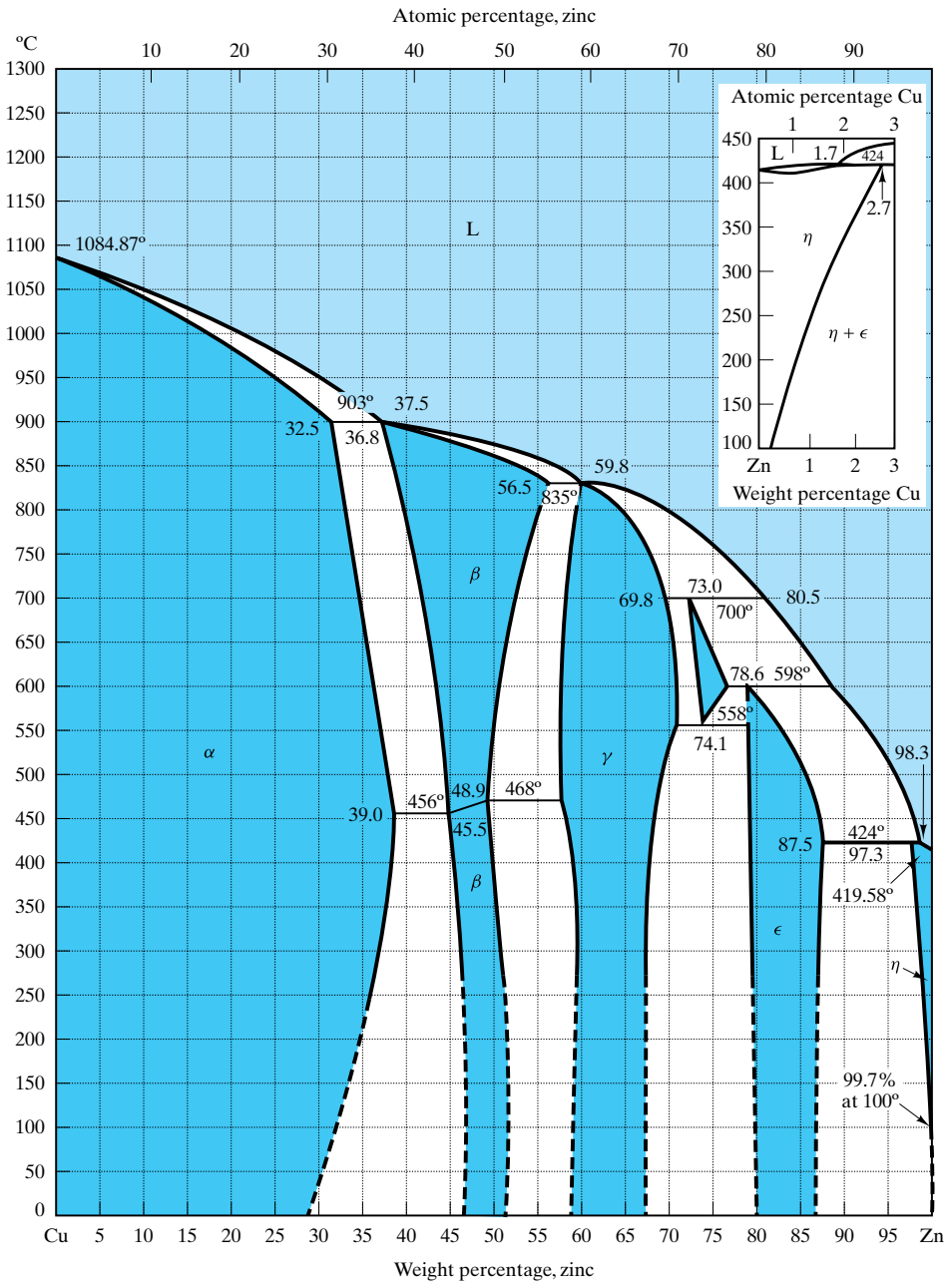

Figure 9-29 *Cu–Zn phase diagram. (After* Metals Handbook, *8th ed., Vol. 8:* Metallography, Structures, and Phase Diagrams, *American Society for Metals, Metals Park, Ohio, 1973, and* Binary Alloy Phase Diagrams, *Vol. 1, T. B. Massalski, ed., American Society for Metals, Metals Park, Ohio, 1986.)*

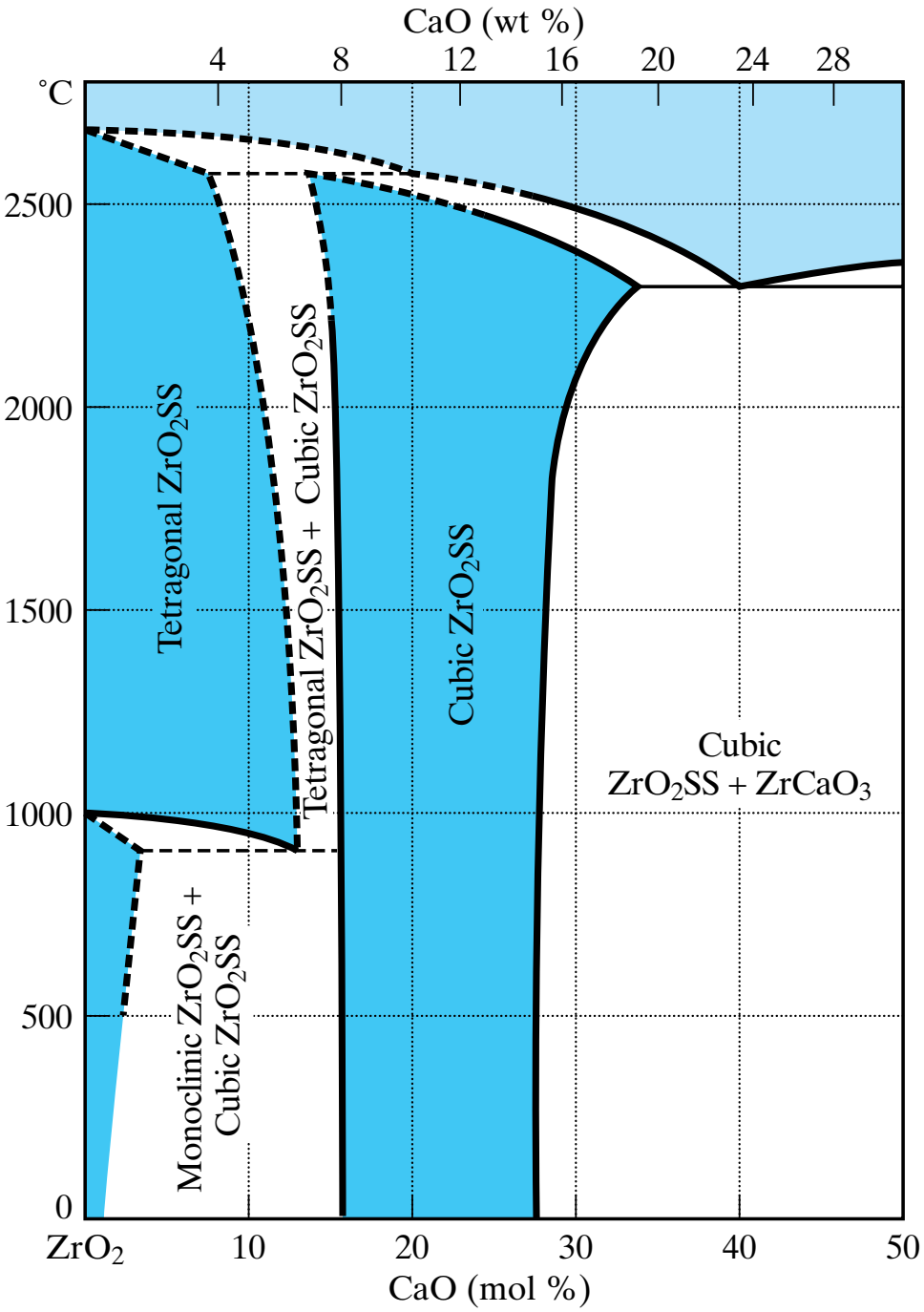

Figure 9-30 *$CaO–ZrO_2$ phase diagram. The dashed lines represent tentative results. (After* Phase Diagrams for Ceramists, *Vol. 1, American Ceramic Society, Columbus, Ohio, 1964.)*

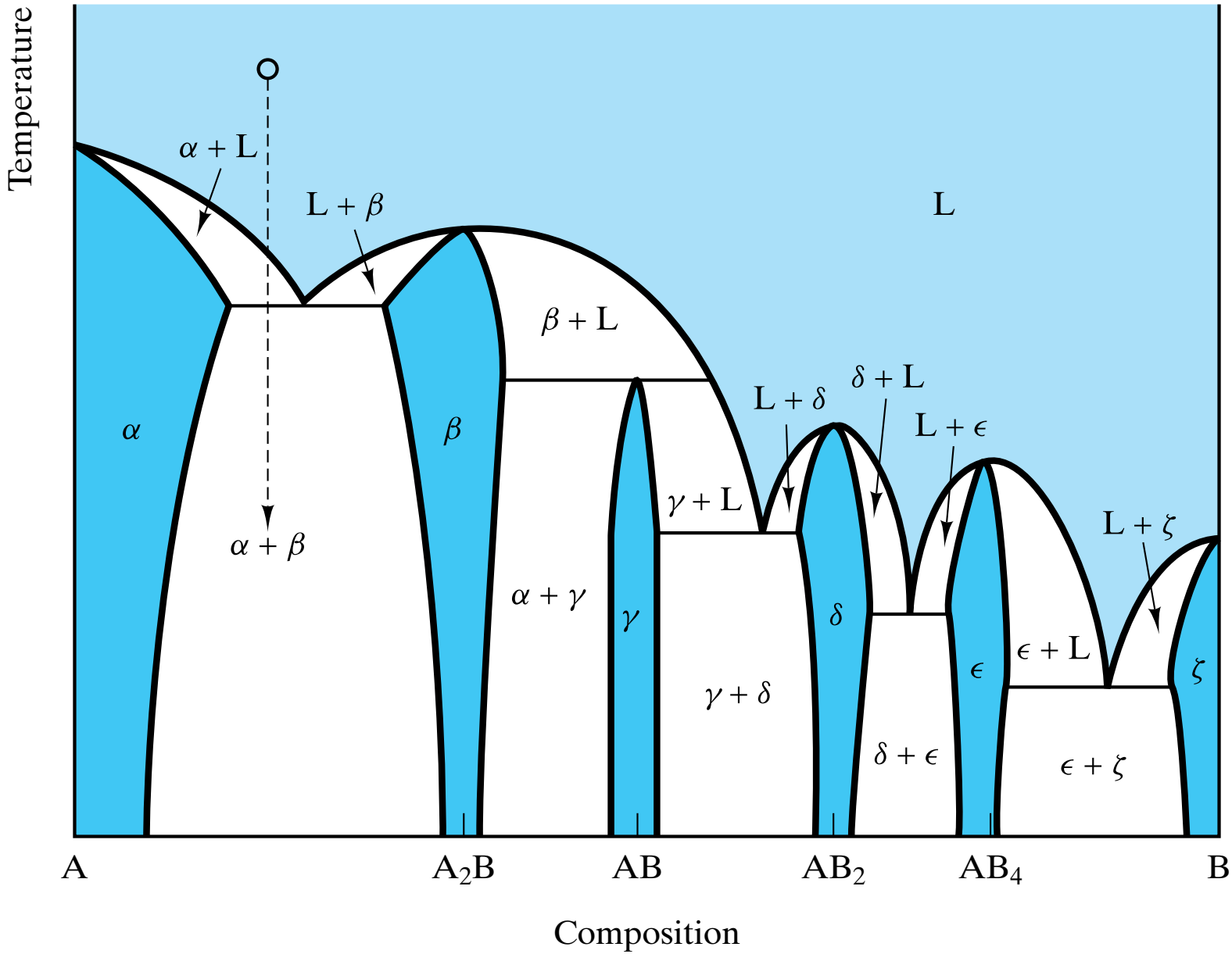
Temperature
α + L
L + β
L
β + L
α
β
L + δ
δ + L
L + ϵ
γ + L
L + ζ
α + β
α + γ
γ
δ
ϵ
ϵ + L
ζ
γ + δ
δ + ϵ
ϵ + ζ
A
A2B
AB
AB2
AB4
B
Composition

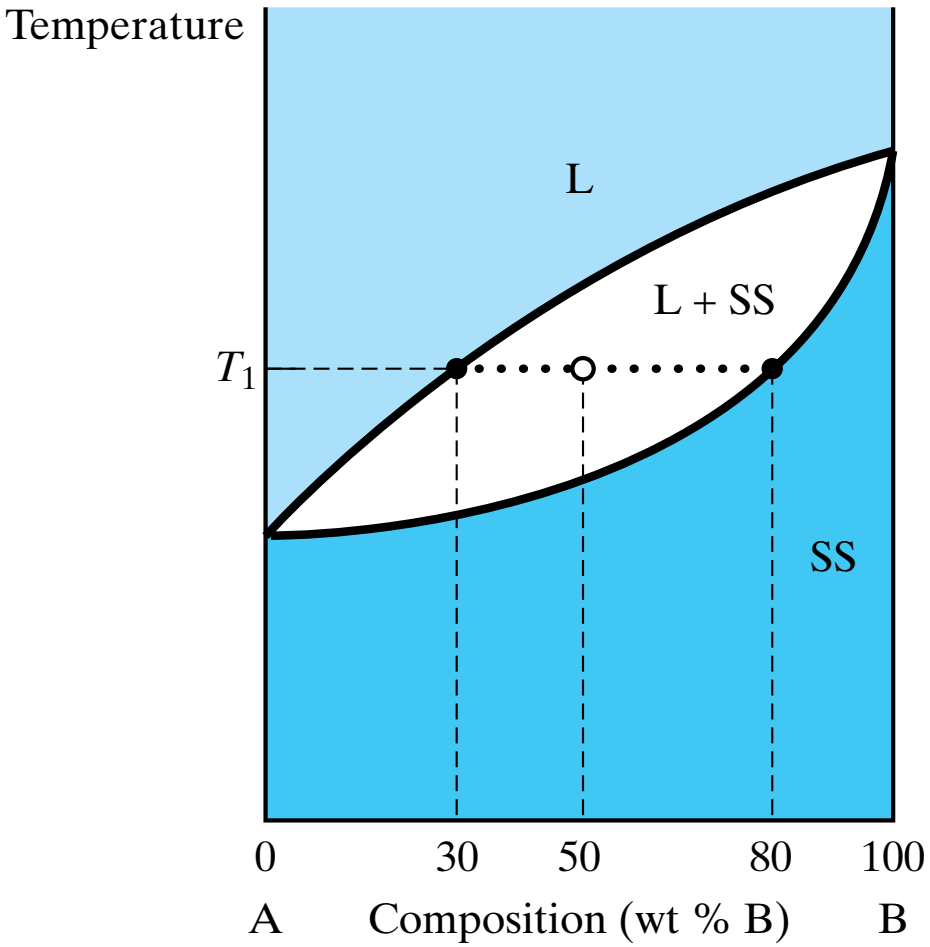

$$m_L + m_{SS} = m_{total}$$
$$0.30m_L + 0.80m_{SS} = 0.50m_{total}$$
$$\rightarrow m_L = 0.60m_{total}$$
$$m_{SS} = 0.40m_{total}$$

Figure 9-31 *A more quantitative treatment of the tie line introduced in Figure 9–6 allows the amount of each phase (L and SS) to be calculated by means of a mass balance (Equations 9.6 and 9.7).*

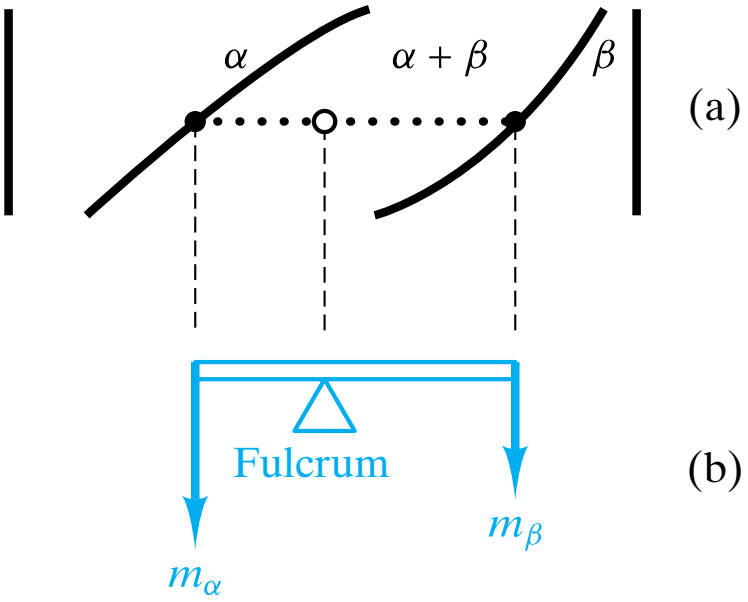

Figure 9-32 *The lever rule is a mechanical analogy to the mass balance calculation. The (a) tie line in the two-phase region is analogous to (b) a lever balanced on a fulcrum.*

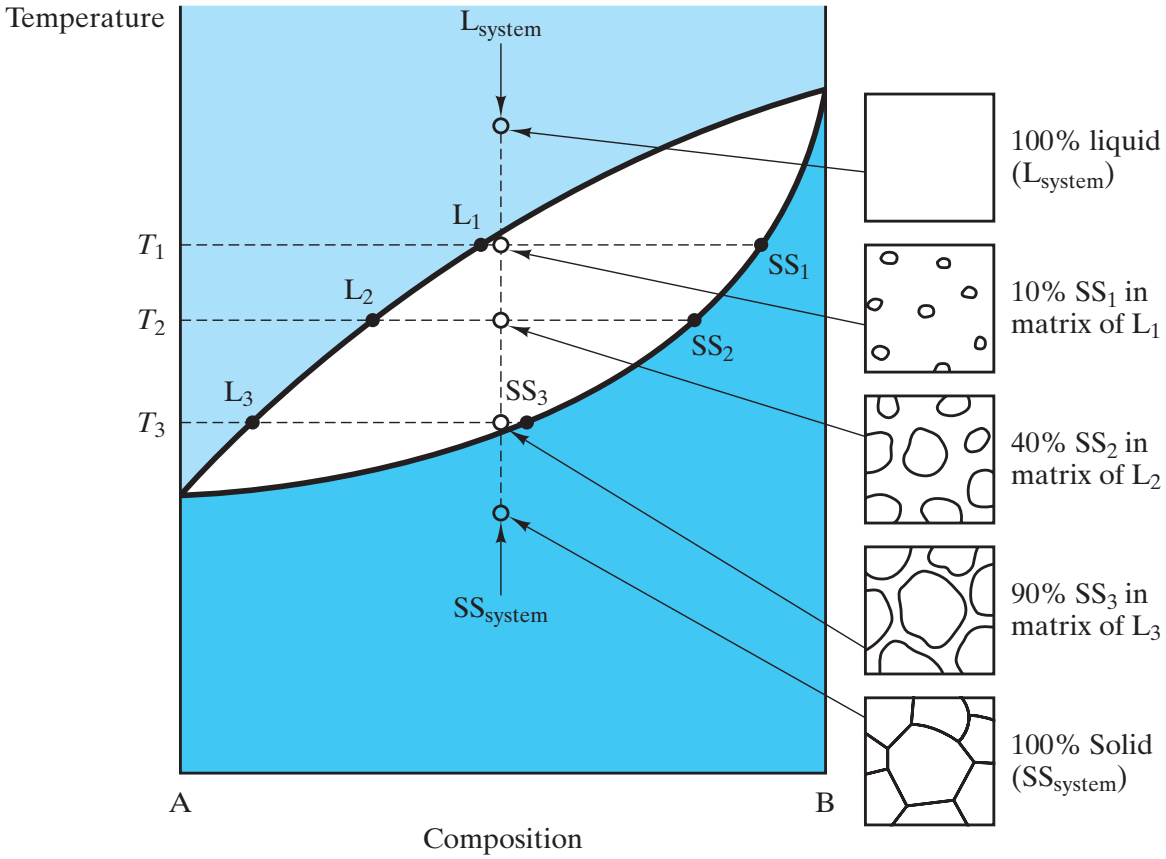

Figure 9-33 *Microstructural development during the slow cooling of a 50% A–50% B composition in a phase diagram with complete solid solution. At each temperature, the amounts of the phases in the microstructure correspond to a lever rule calculation. The microstructure at T_2 corresponds to the calculation in Figure 9–31.*

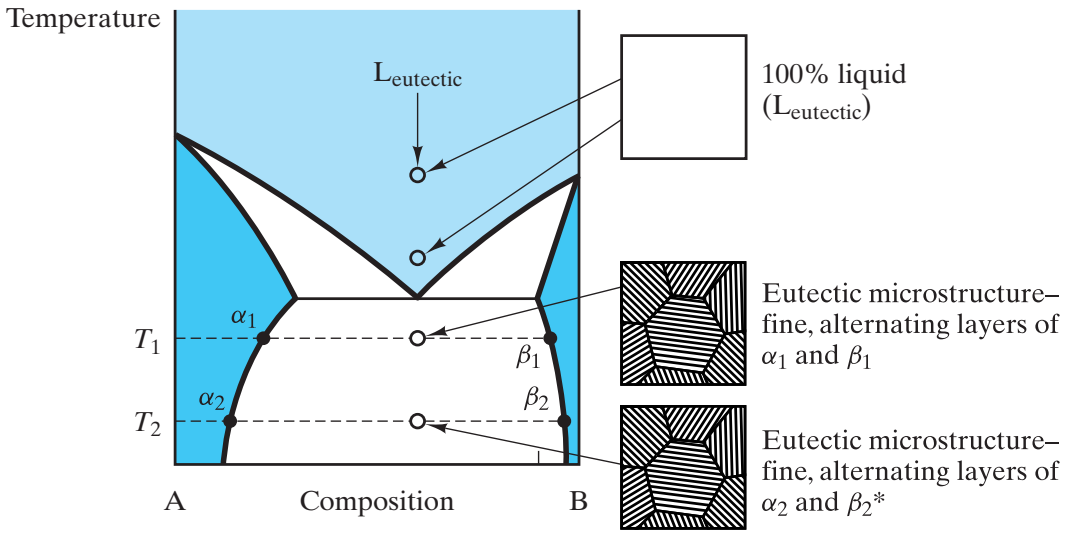

*The only differences from the T_1 microstructure are the phase compositions and the relative amounts of each phase. For example, the amount of b will be proportional to

$$\frac{x_{eutectic} - x_\alpha}{x_\beta - x_\alpha}$$

Figure 9-34 *Microstructural development during the slow cooling of a eutectic composition.*

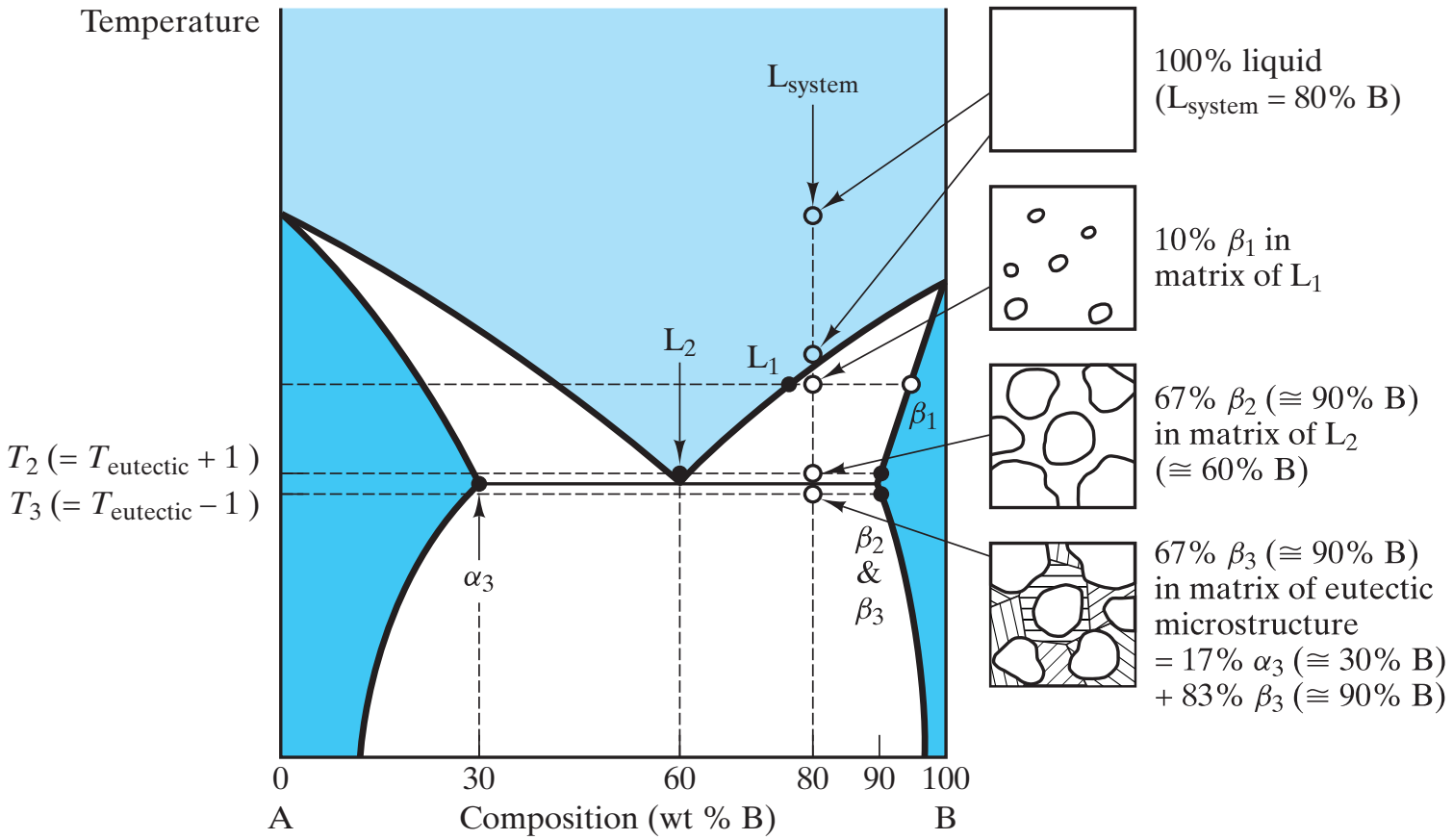

Figure 9-35 *Microstructural development during the slow cooling of a hypereutectic composition.*

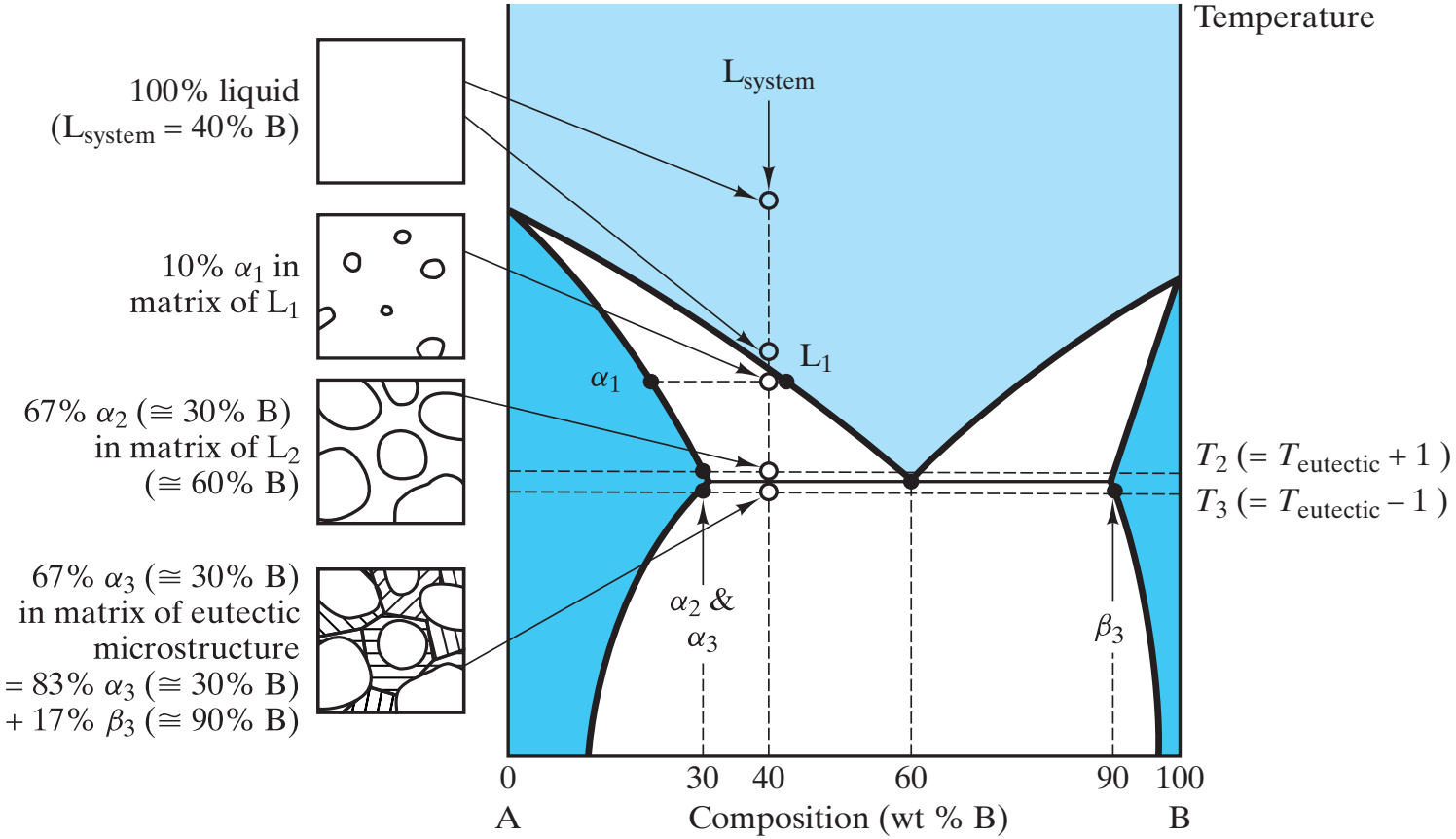

Figure 9-36 *Microstructural development during the slow cooling of a hypoeutectic composition.*

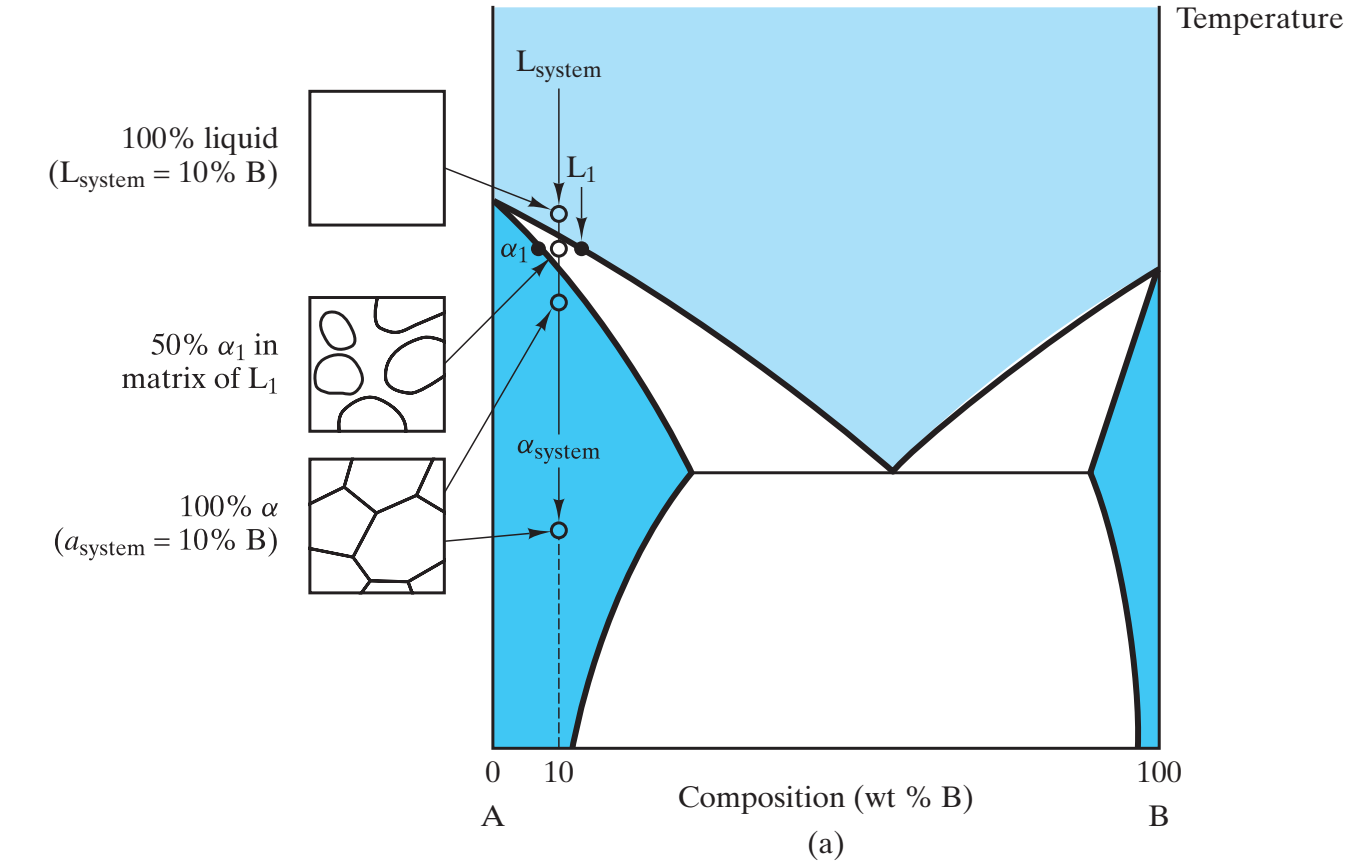
Temperature
L_{system}
L_1
α_1
α_{system}
100% liquid
(L_{system} = 10% B)
50% α_1 in
matrix of L_1
100% α
(a_{system} = 10% B)
0
10
100
A
Composition (wt % B)
B
(a)

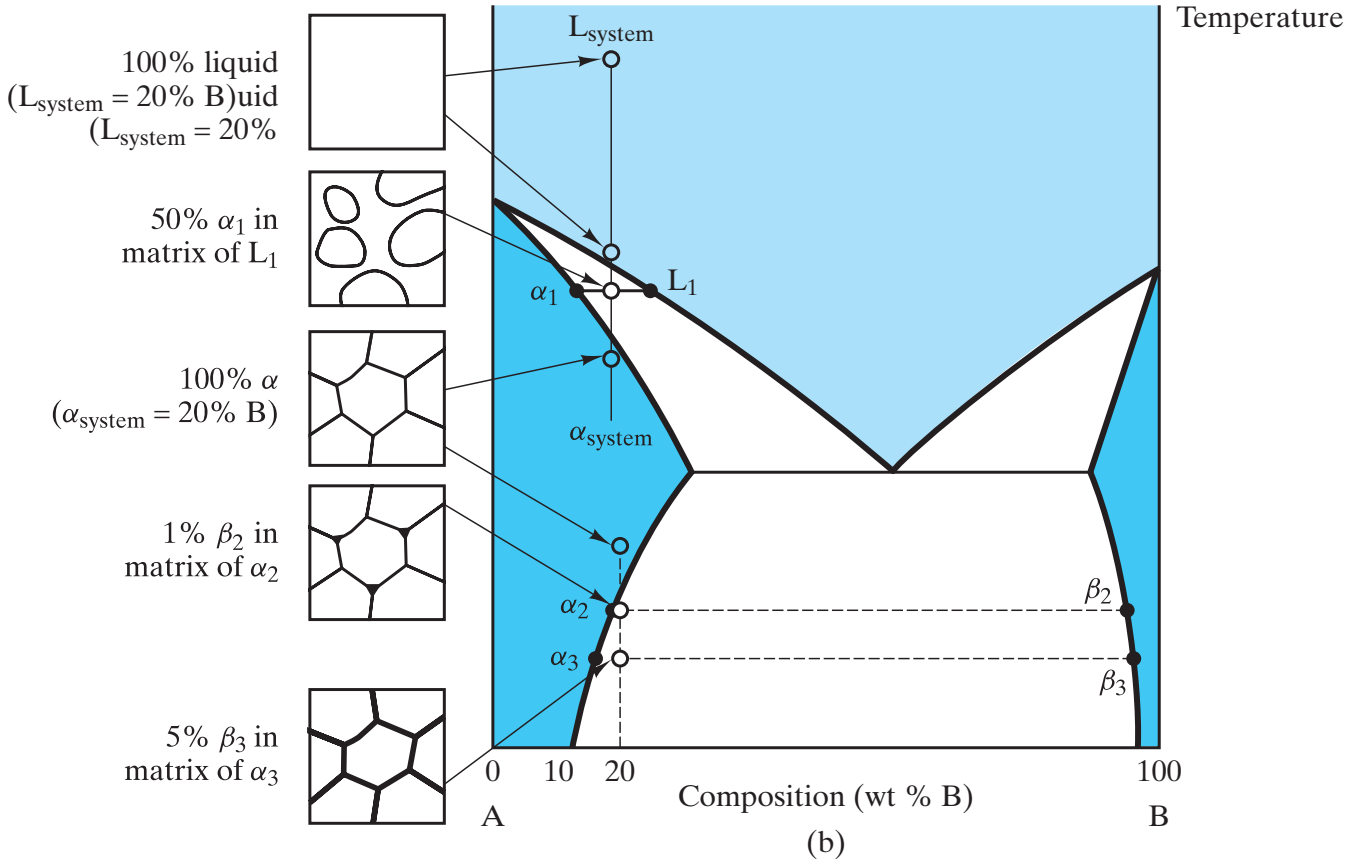
Temperature
L_{system}
L_1
α_1
α_{system}
β_2
β_3
α_2
α_3
100% liquid
(L_{system} = 20% B)uid
(L_{system} = 20%
50% α_1 in
matrix of L_1
100% α
(α_{system} = 20% B)
1% β_2 in
matrix of α_2
5% β_3 in
matrix of α_3
0
10
20
100
A
Composition (wt % B)
B
(b)

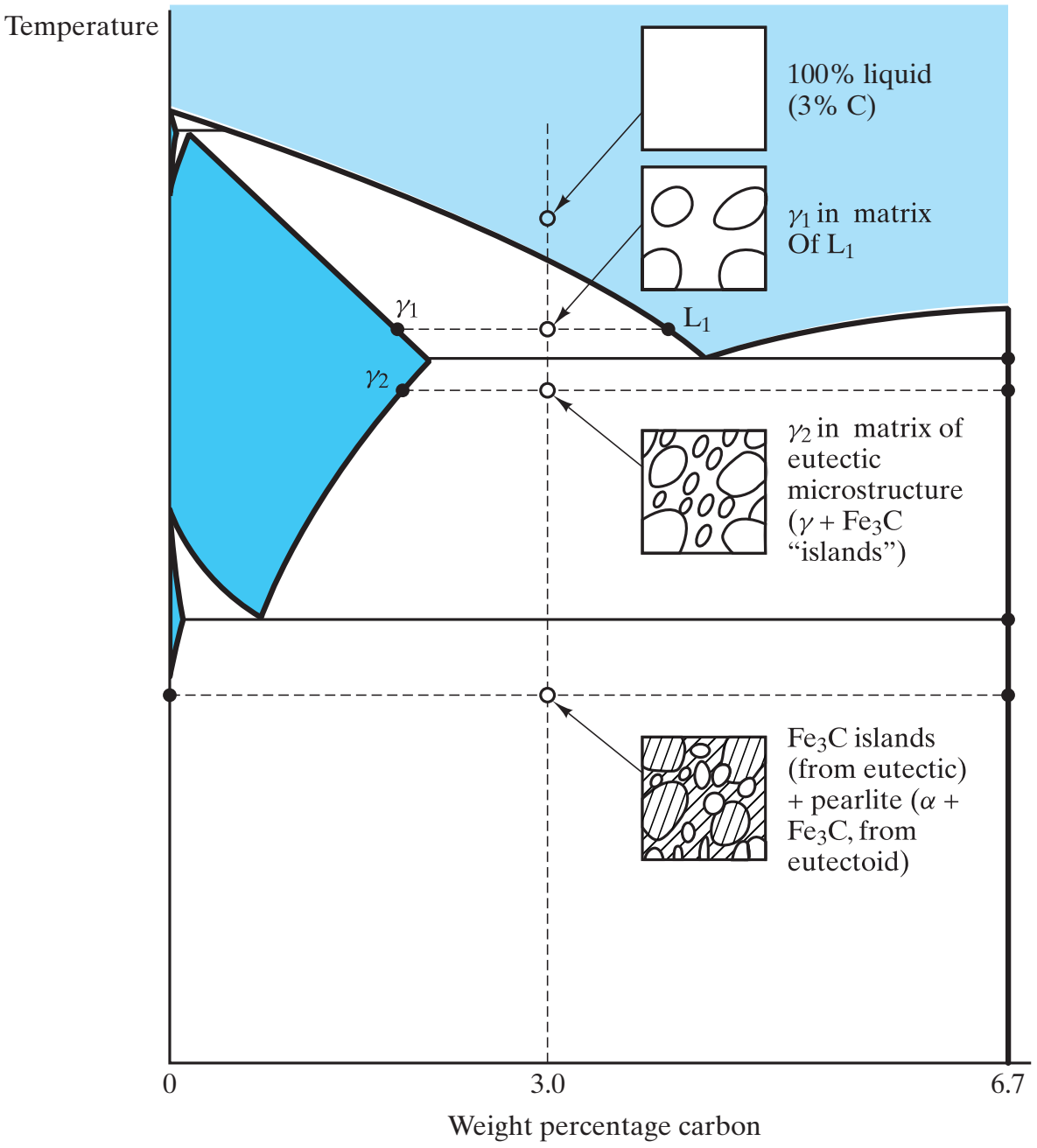

Figure 9-38 *Microstructural development for white cast iron (of composition 3.0 wt % C) shown with the aid of the Fe–Fe_3C phase diagram. The resulting (low-temperature) sketch can be compared with a micrograph in Figure 11–1a.*

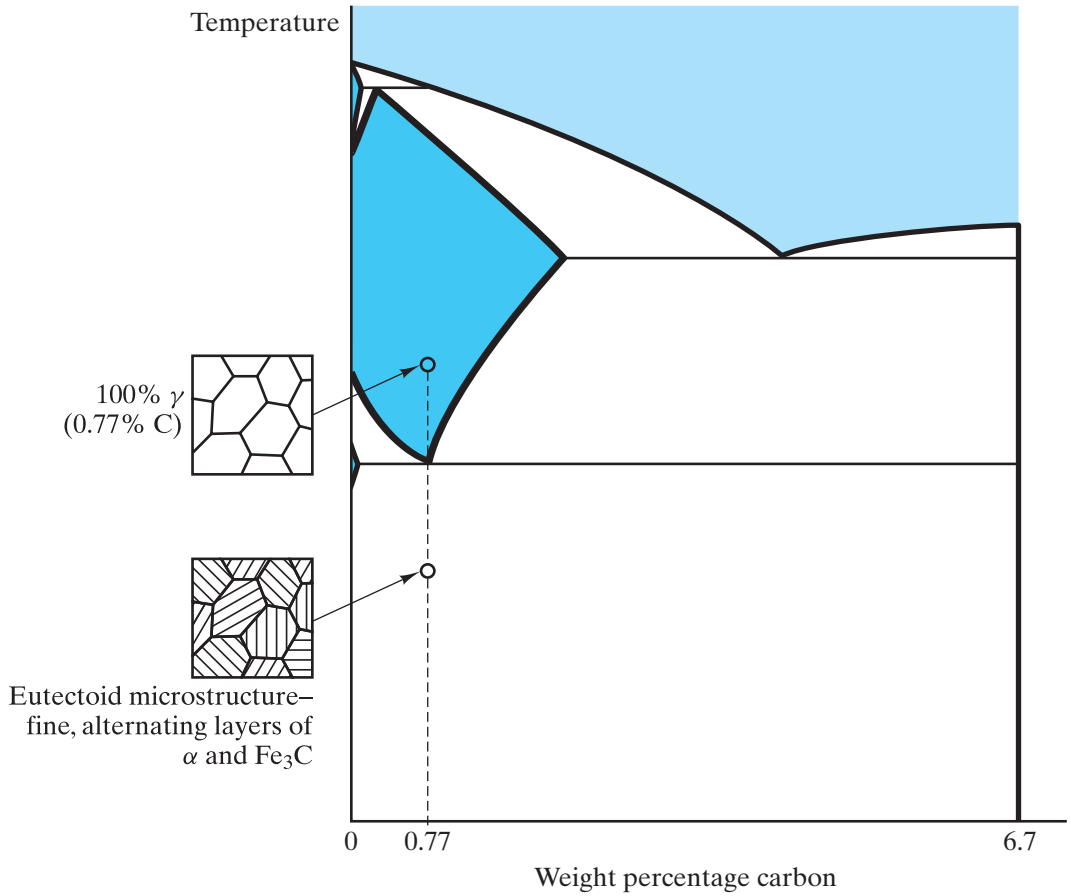

Figure 9-39 *Microstructural development for eutectoid steel (of composition 0.77 wt % C). The resulting (low-temperature) sketch can be compared with the micrograph in Figure 9–2.*

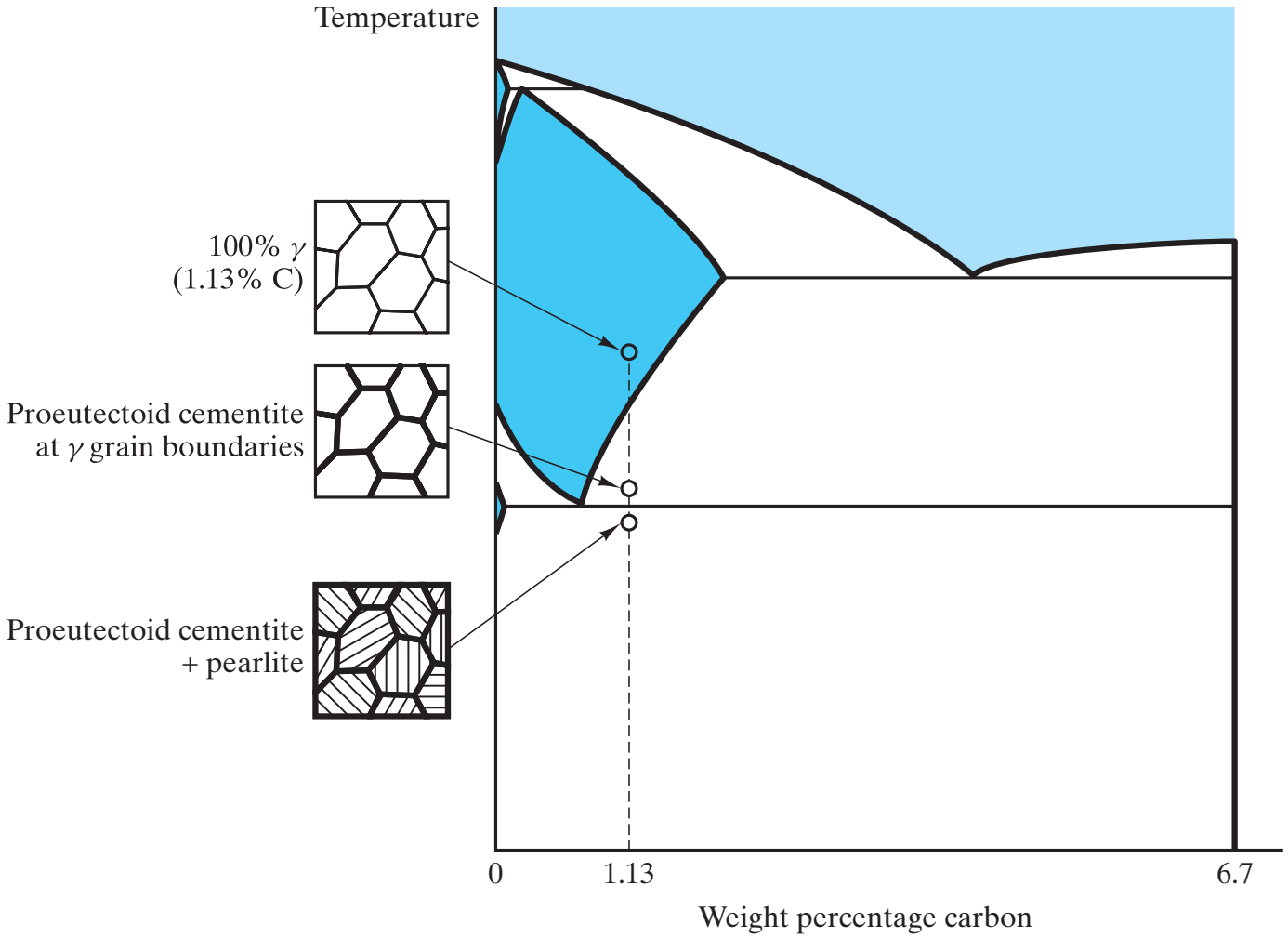

Figure 9-40 *Microstructural development for a slowly cooled hypereutectoid steel (of composition 1.13 wt % C).*

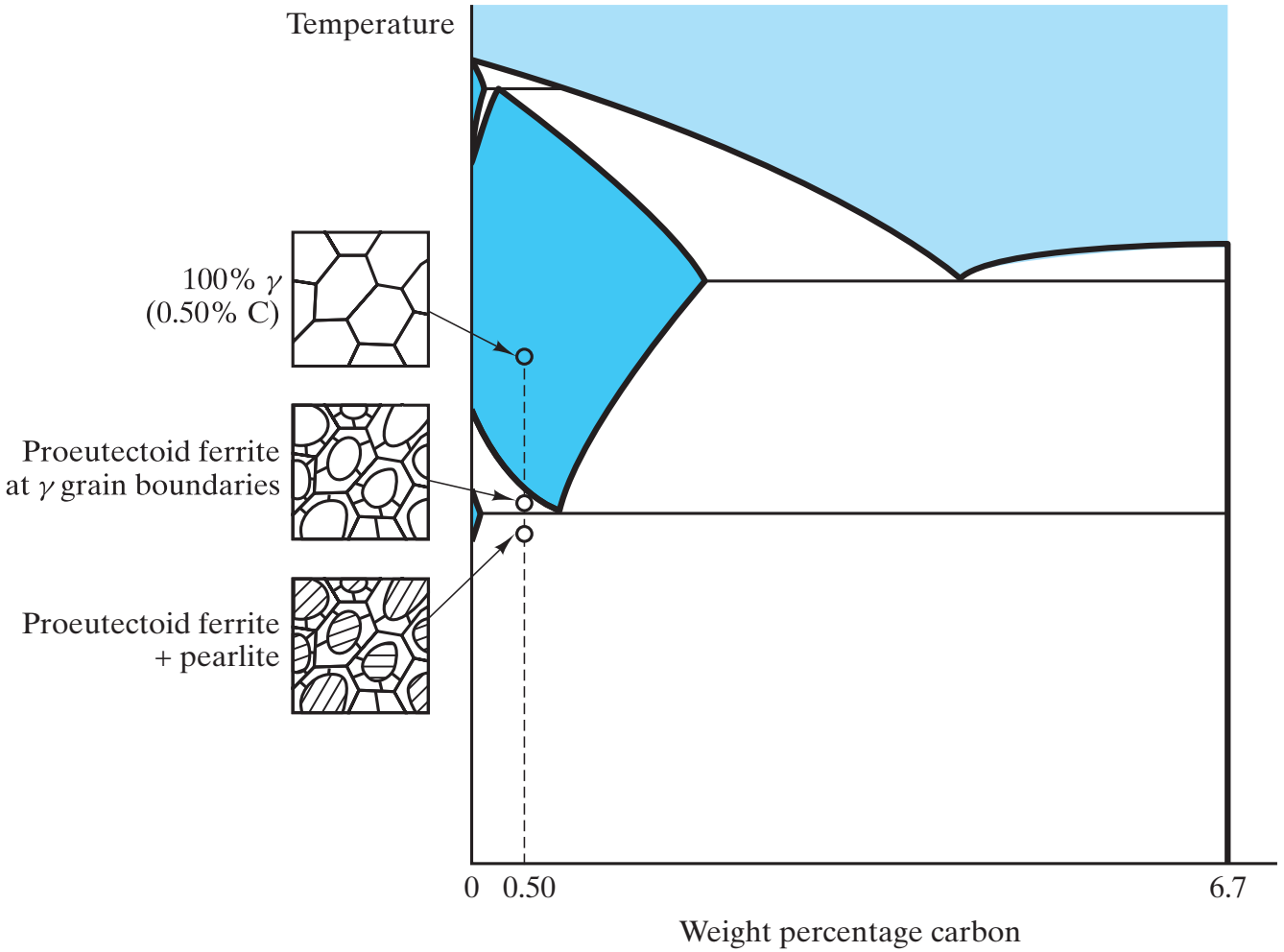

Figure 9-41 *Microstructural development for a slowly cooled hypoeutectoid steel (of composition 0.50 wt % C).*

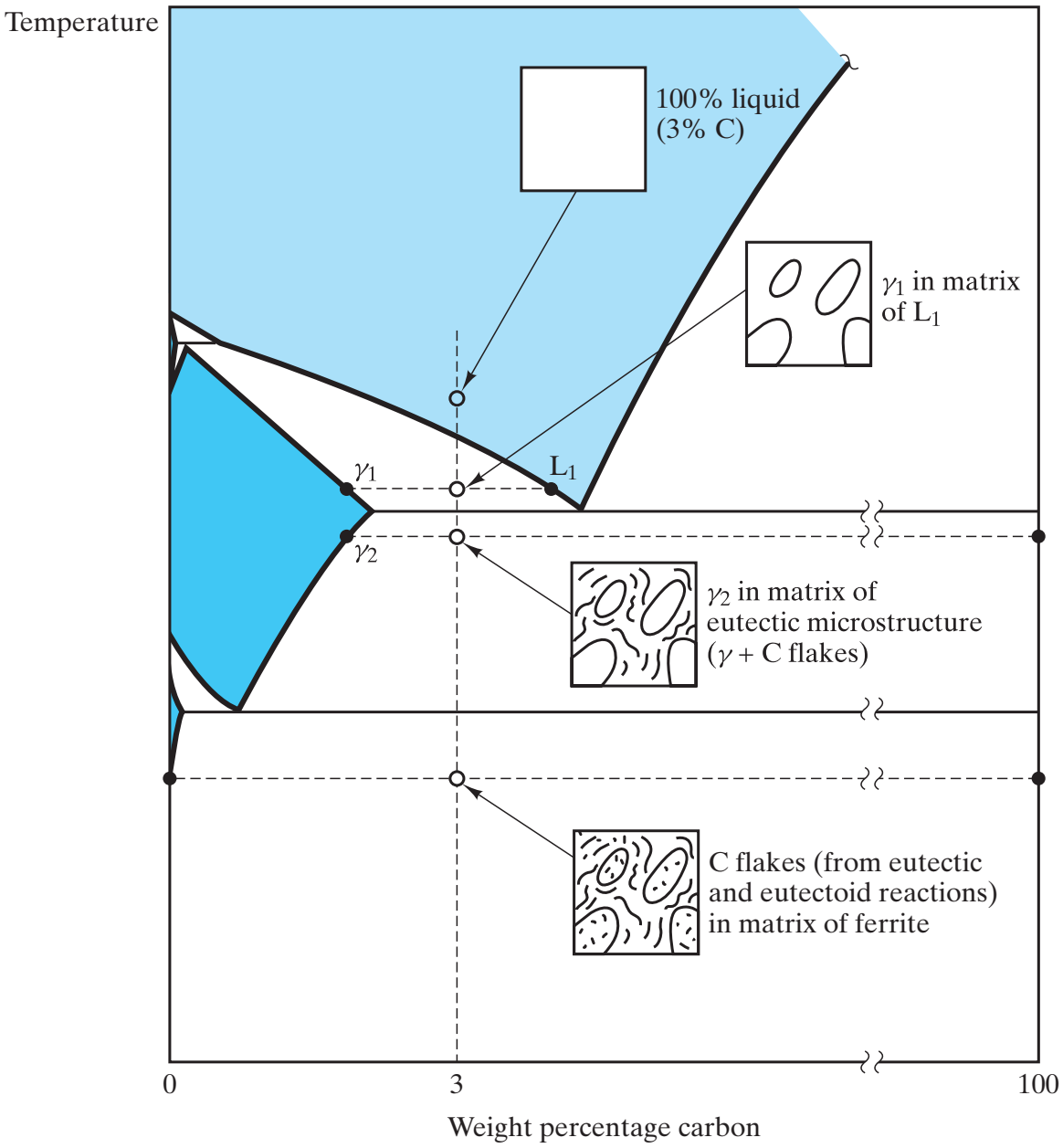

Figure 9-42 *Microstructural development for gray cast iron (of composition 3.0 wt % C) shown on the Fe–C phase diagram. The resulting low-temperature sketch can be compared with the micrograph in Figure 11–1b. A dramatic difference is that, in the actual microstructure, a substantial amount of metastable pearlite was formed at the eutectoid temperature. It is also interesting to compare this sketch with that for white cast iron in Figure 9–38. The small amount of silicon added to promote graphite precipitation is not shown in this two-component diagram.*

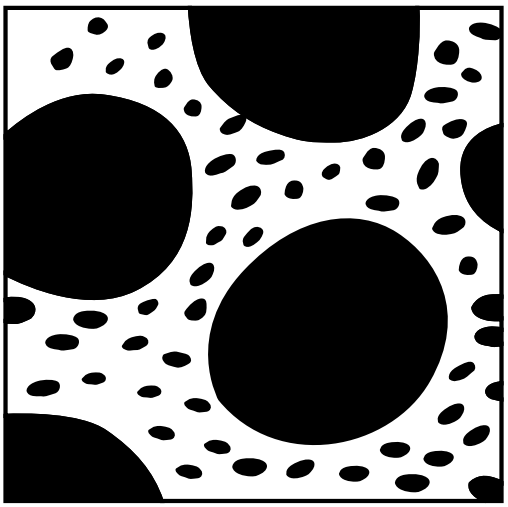

The phase diagram for this alloy system is